CellPress

Trends in Biotechnology

Research Article

Automated adjustment of metabolic niches enables the control of natural and engineered microbial co-cultures

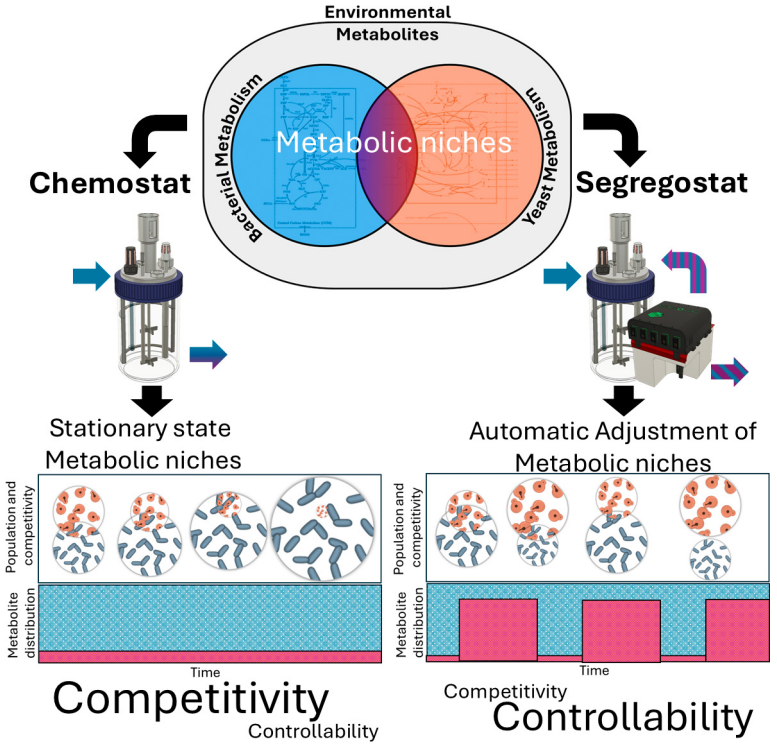

The study introduces 'automated adjustment of metabolic niches' (AAMN), a feedback control method using substrate pulsing to stabilize co-cultures. AAMN enables control by promoting organism diversification to alternative metabolic niches. AAMN was proven effective during continuous bioproduction of p-coumaric acid, resulting in novel insights into microbial interactions within bioprocessing applications.

Juan Andres Martinez, Romain Bouchat, Tiphaine Gallet de Saint Aurin, MartinezLuz María Martínez, Luis Caspeta, Samuel Telek, Andrew Zicler, Guillermo Gosset, Frank Delvigne

F.Delvigne@uliege.be (F. Delvigne).

Highlights

The competitive exclusion principle states that a single metabolic niche (MN) can support the growth of only one species in continuous cultivation.

Alternating MNs at an adequate frequency can support the growth of yeast–bacteria co-cultures.

Automated adjustment of metabolic niches (AAMN) based on a cell–machine interface, allows for the stabilization of either cooperative or competitive co-cultures.

AAMN enables the continuous bioproduction of p-coumaric acid by an engineered yeast–bacteria co-culture exhibiting division of labor.

Trends in Biotechnology, Month 2024, Vol. xx, No. xx
https://doi.org/10.1016/j.tibtech.2024.12.005>

Trends in Biotechnology

CellPress

Research Article

Automated adjustment of metabolic niches enables the control of natural and engineered microbial co-cultures

Juan Andres Martinez [1], Romain Bouchat [1], Tiphaine Gallet de Saint Aurin [1], Luz María Martínez [2], Luis Caspeta [2], Samuel Telek [1], Andrew Zicler [1], Guillermo Gosset [2], and Frank Delvigne [1,*]

Much attention has focused on understanding microbial interactions leading to stable co-cultures. In this work, substrate pulsing was performed to promote better control of the metabolic niches (MNs) corresponding to each species, leading to the continuous co-cultivation of diverse microbial organisms. We used a cell–machine interface, which allows adjustment of the temporal profile of two MNs according to a rhythm, ensuring the successive growth of two species, in our case, a yeast and a bacterium. The resulting approach, called 'automated adjustment of metabolic niches' (AAMN), was effective for stabilizing both cooperative and competitive co-cultures. AAMN can be considered an enabling technology for the deployment of co-cultures in bioprocesses, demonstrated here based on the continuous bioproduction of p-coumaric acid. The data accumulated suggest that AAMN could be used not only for a wider range of biological systems, but also to gain fundamental insights into microbial interaction mechanisms.

Introduction

Ensuring the coexistence of several microbial species in the same cultivation device would be an important technological advance, in terms of both fundamental research (e.g., understanding how species can coexist and what are the ecological drivers for this coexistence [1–4]), and applications (e.g., through the exploitation of division of labor for bioproduction [5–7]). The coexistence of microbial species is hampered by the competitive exclusion principle, but it is possible to overcome this in several cases by providing access to alternative **MNs** (see Glossary) [8]. The MN is the set of abiotic factors leading to the growth performance of a given species (i.e., substrate, temperature, and pH) [9,10]. A simple way to diversify the MN is by adding nutrients into the cultivation device [11,12]. However, simple addition is not enough to ensure coexistence or population stability as we need to take into account the particular dynamics of each biological system (i.e., growth, substrate diversification, and other sources of metabolic heterogeneity) [13–15]. By pulsing only one type of nutrient (e.g., carbon source), it is possible to generate a temporal succession of MNs through overflow metabolism and diauxic shift regulation, leading to the successive growth of the different species in the co-culture [8]. However, determination of the amplitude and frequency to be considered is not straightforward and depends on, among other factors, the global environmental conditions and microbial species under consideration. In addition, depending on the degree of cooperation between the microbial species, environmental perturbation can lead to unexpected effects, such as increased stability for the most cooperative co-cultures or decreased stability for highly competitive co-cultures [2].

Technology readiness

The Segregostat approach combines the monitoring of microbial populations by online flow cytometry analysis, and the control of their response by tailored control rules and actuators (i.e., pulses of different metabolites). It was initially developed to monitor and mitigate the impact of microbial population heterogeneity on bioprocess robustness. The current version of the Segregostat, including its hardware interface and software, has led to the production of different protocols to control gene expression, biofilm production, automated pulsing of diverse substrates to promote bioprocess population homogeneity and productivity, and finally the automated adjustment of metabolic niches (AAMN) for the control of co-cultured populations [technology readiness level (TRL) 6]. Several areas of opportunity remain, such as signal multiplexing, adaptive control rules based on models and or artificial intelligence (AI), and its implementation to pilot-scale to achieve TRL 7. However, during the 11 years of Segregostat development, we have been able to continuously prove its abilities to increase bioprocess robustness by understanding and controlling the dynamics of cell diversification processes.

[1]Terra Research and Teaching Centre, Microbial Processes and Interactions (MiPI), Gembloux Agro-Bio Tech, University of Liège, Gembloux, Belgium
[2]Departamento de Ingeniería Celular y Biocatálisis, Instituto de Biotecnología, Universidad Nacional Autónoma de México, Morelos, Cuernavaca, Mexico

*Correspondence:
F.Delvigne@uliege.be (F. Delvigne).

In a previous study, we investigated the impact of environmental perturbations on the stability of a highly competitive co-culture involving *Saccharomyces cerevisiae* (SAC) and *Escherichia coli* (ECO) in a continuous cultivation device [13]. In a conventional MN, where glucose was the main carbon source, the competitive exclusion principle led to progressive exclusion of the slow grower (SAC) and dominance of the fast grower (ECO). However, following the diauxic shift onto alternative substrates released by overflow metabolism [i.e., ethanol (ETH) and acetate (ACE)], SAC transiently exhibited higher fitness. Cross-feeding based on overflow metabolites is known to promote community stabilization [2,16]. We exploited this MN by applying glucose pulsing at specific frequencies and amplitudes. For this purpose, we developed a model called **Monod-type co-culture kinetic simulation (MONCKS)**, involving individual Monod-based models for each species. A **cybernetic modeling (CM)** approach was used to estimate the substrate utilization for each species in function of the appearance of the MNs, with growth rate as the metabolic optimization target. In this way, we were able to both simulate, and experimentally verify, several scenarios for the coexistence of yeast and bacteria. While effective, this approach did not enable us to obtain a co-culture with an equal number of individuals of both species, mainly because the model only considered a limited number of metabolic states to transform substrates to biomass and byproducts. In addition, the number of possible bioprocessing scenarios that can be simulated by MONCKS was too high to be tested experimentally.

The current study relies on the concept of ecological niches or MNs, and the abilities of the co-cultured microorganisms to explore and diversify toward utilizing these niches. Typically, the maintenance of a single MN promotes the dominance of one microbial species over the others. Thus, to ensure the coexistence of two microbial species, a dynamic correlation is necessary between the size of at least two distinct MNs at a frequency that is compatible with the growth capabilities of each species. Here, we adapted a cell–machine interface for automatically adjusting the transition between selected MNs and ensuring the coexistence of different types of yeast–bacteria co-culture exhibiting different mechanisms of interaction, an approach called **AAMN**. The success of this operation is not straightforward since the MNs can exhibit overlaps and variation in time (i.e., niche expansion and contraction) [2,17,18]. In addition, it is not easy to precisely define a MN more specifically when complex microbial interactions are involved. Indeed, microorganisms diversify by exploiting novel metabolic pathways and unoccupied MNs, allowing them to thrive in their environment. This process of metabolic innovation enables species to adapt to changing conditions, outcompete rivals, and occupy new ecological roles [19,20].

We then further expanded the MONCKS toolbox to directly integrate publicly available metabolic network models as a predictive tool for the optimization of the cell–machine interface. Several studies have pointed out that a MN can be captured more efficiently based on a quantitative biology approach using concepts derived from metabolic flux analysis [17–23]. Based on these models, we observed that MNs overlapped for all the co-cultures involved in this work, but stability could be reached based on AAMN due to either metabolite cross-feeding or the precise timing for the adjustment of MNs. Finally, based on these observations, we successfully implemented AAMN for the continuous bioproduction of p-coumaric acid, an important building block for chemical synthesis [24].

Glossary

Automated adjustment of metabolic niches (AAMN): closed-control loop operation of a co-culture in which actuator pulses of substrate modify the temporal availability of the MNs to stabilize specific population compositions.
Cybernetic modeling (CM): metabolic modeling approach that uses dynamic cybernetic functions to calculate regulatory processes within cellular metabolism. It uses matching law mathematical relationships between a metabolic objective (i.e., maximizing growth rate) to reinforce or relax different elementary modes and, therefore, approximate the instantaneous metabolic flux distributions, either for internal or externalized metabolites.
Elementary mode (EM): minimal indivisible flux path derived from the stoichiometry matrix analysis. Each one represents a metabolic flux distribution. The total set comprises the metabolic capabilities of the organism and the active set comprises the metabolic flux distributions that are able to be used by the organism in a particular environmental conditions.
Entropy (H): Information Theory Entropy; quantifies the average level of uncertainty of a random variable in terms of the variables potential states or outcomes. In this case, it calculates the amount of dispersion of an organism in terms of the potential phenotypes, by calculating the uncertainty of finding each metabolic behavior phenotype.
Metabolic niche (MN): set of environmental conditions and metabolic capabilities of an organism that can lead to population growth or persistence. In this case, it refers to the substrate produced or added to the bioreactor at a rate that can enable population growth or persistence.
Monod-type co-culture kinetic simulation (MONCKS): specialized form of CM solved by numeric approximation that is performed around two or more organisms in co-culture, each with its own active set of elementary modes and cybernetic regulators.

Results

AAMN as a generic strategy for the stabilization of cooperative and competitive co-cultures

The succession of two MNs at an appropriate frequency can be used as a generic strategy for stabilizing the composition of a co-culture [8,11,20,25,26]. Accordingly, we designed a cell–machine interface that automatically triggered the addition of substrate pulses based on the composition of the co-culture (Figure 1A). This interface comprises an automated flow cytometer (FC)

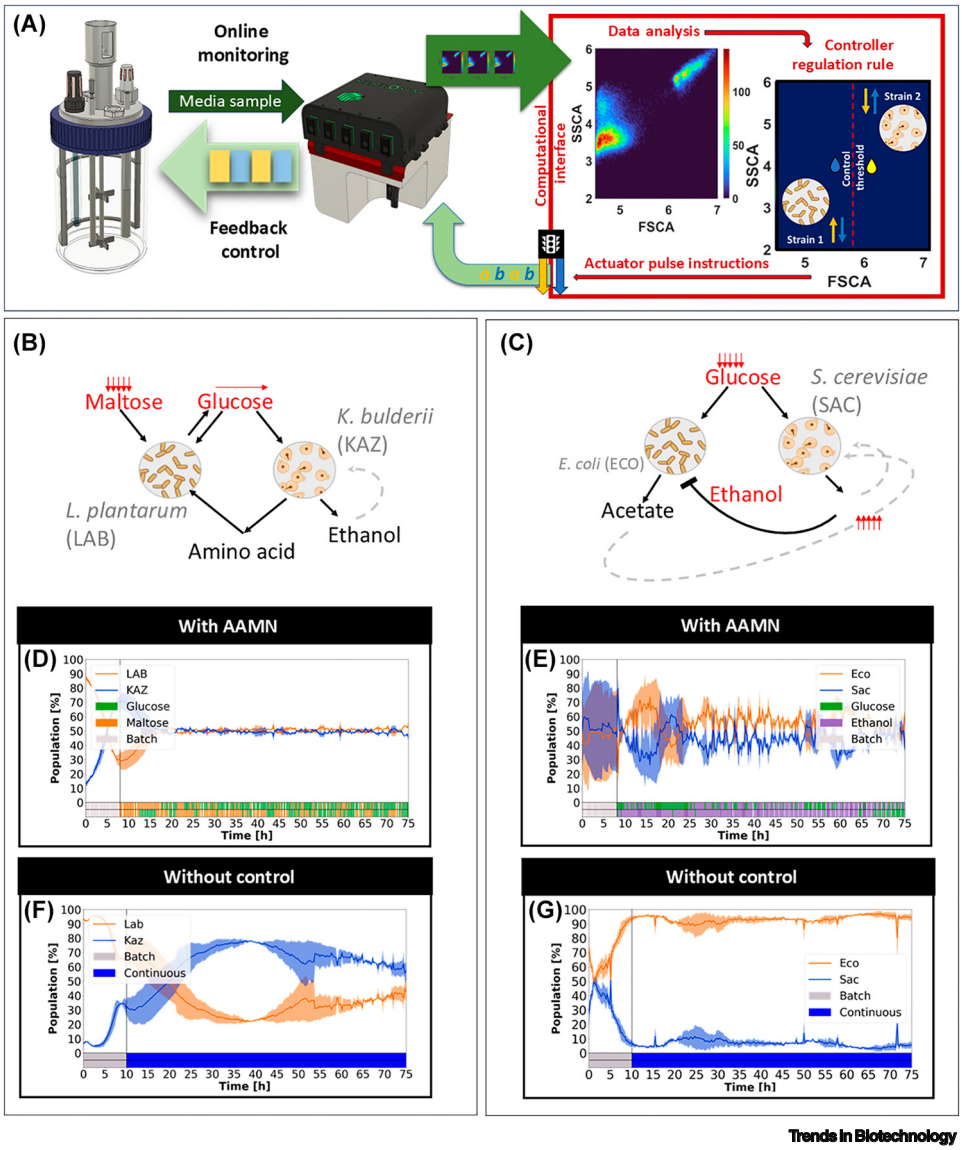

Figure 1. Automated reversion of metabolic niches (MNs) can be used for stabilizing either cooperative or competitive co-cultures. (A) Cell–machine interface relying on automated flow cytometry (FC) allows for the control of co-culture composition (50%–50% for each species is selected here as a setpoint). Briefly, samples are taken automatically and diluted before being analyzed by FC. Based on the analysis of the forward (FSC-A) and side (SSC-A) scatter signals, bacterial and yeast cells can be easily distinguished from each other. When the setpoint is not fulfilled, pulses of substrates (the nature of the substrate depends on the biological systems considered) are applied to restore the equal abundance between the species. (B,C) Schematic of the metabolic interactions between (B) *Lactiplantibacillus plantarum* (LAB) and *Kazachstania bulderii* (KAZ) and (C) *Escherichia coli* (ECO) and *Saccharomyces cerevisiae* (SAC). The red arrows indicate whether the substrate is provided by pulses or continuously during the cultivation. (D,E) Evolution of the number of cells (as determined based on automated FC) for a (D) LAB-KAZ co-culture and (E) ECO-SAC co-culture in a continuous cultivation device with automated adjustment of metabolic niches (AAMN; nutrient pulsing profile at the bottom of each figure is shown for n = two biological replicates). (F,G) Evolution of the number of cells (as determined based on automated FC) for (F) a LAB-KAZ co-culture and (G) an ECO-SAC co-culture in a chemostat without AAMN. All cultivations were performed in duplicate (n = 2).

[27], which allows the culture to be sampled at regular time interval (i.e., every 15 min). The forward (FSC-A) and side-scatter (SSC-A) channels are used to discriminate between yeast and bacterial cells based on their size/morphology. In our case, a control was applied to ensure

an equal abundance of each species (i.e., 50% yeast and 50% bacteria) during continuous cultivation. Based on this simple rule, a pulse of carbon source compatible with one of the species was triggered when its abundance increased >50%. We applied a similar approach previously for controlling phenotypically different subpopulations in monocultures based on a cultivation device called the Segregostat and involving reactive flow cytometry for promoting a specific population state [28,29]. To estimate the potential of our AAMN approach to be generalized for diverse biological systems, we started the experiments based on two types of yeast–bacteria co-culture differing at the level of their microbial interaction mechanisms.

The first candidate was a co-culture involving *Kazakstania bulderii* (a yeast, KAZ) and *Lactiplantibacillus plantarum* (a lactic acid bacteria, LAB), a combination typically found in sourdough [30] (Figure 1B). This type of co-culture exhibits several commensalism interactions, with the yeast providing resources (amino acids and nucleic acids) to the LAB [31,32]. During the implementation of AAMN for stabilizing KAZ-LAB, we also pulsed glucose to the co-culture. The maltose provided by the continuous feeding cannot be consumed by KAZ, but can be partially assimilated by LAB, with one molecule of glucose being phosphorylated and assimilated by LAB, and the other molecule being released into the extracellular medium [33,34]. The released glucose can then be utilized by KAZ, leading to a double cross-feeding system that promotes co-culture stability [35–37]. The second co-culture considered involved SAC CEN.PK 113-7D and ECO W3110 (Figure 1C). This co-culture exhibited more complex competitive/commensalism interactions, notably all the excretion of overflow and/or fermentation metabolites (i.e., mainly ETH and ACE) that can act as alternative carbon sources and promote cross-feeding, competition, and even exclusion by inhibitory effects. Taken together, these alternative metabolic pathways determine the establishment of the appropriate MNs.

We previously demonstrated that it is possible to stabilize co-cultures (20% SAC; 80% ECO) based on periodic pulsing of glucose [13]. Under these conditions, ECO exhibited the highest fitness when glucose concentration was high, but SAC exhibited higher fitness at a low glucose concentration and following reassimilation of ACE and ETH. The pulsing frequency was predicted based on a cybernetic model and several scenarios, with different levels of co-culture stability, were predicted and experimentally verified [13].

Applying environmental perturbations at given frequencies is effective for the stabilization of co-cultures [12], as well as in more complex microbial communities [11]. However, finding the appropriate perturbation or pulsing frequency is not straightforward. We focused on this aspect by using our cell–machine interface to verify whether the appropriate pulsing frequency can be reached automatically for driving equal composition during the whole continuous cultivation. Taken together, our data show that co-culturing LAB-KAZ (Figure 1D) and ECO-SAC (Figure 1E) based on the AAMN approach leads to stabilization of the co-cultures compared with continuous cultivation performed without control (Figure 1F,G). However, it was more difficult to stabilize the populations of ECO and SAC (Figure 1E) than those of LAB and KAZ (Figure 1D), suggesting that the alternation of MNs is not straightforward in this case. This is mainly because the ECO-SAC system is mostly competing for the substrate, while the LAB–KAZ system can benefit from mutual cross-feeding (i.e., KAZ benefits from the glucose released from maltose by LAB, whereas LAB benefits from the amino acid released from KAZ) (Figure 1B,C). The 50:50 ratio in a number of events relates to higher proportions of SAC in terms of mass. According to this control rule, SAC is then the microorganism consuming most of the glucose available. Later, we consider metabolic and dynamic modeling to simulate the succession of MNs and its impact on co-culture dynamics.

Full reversion of metabolic niches is needed for the stabilization of competitive co-cultures

As described earlier, the LAB-KAZ and ECO-SAC co-cultures displayed different dynamics. For LAB-KAZ, we observe a cooperative behavior whereby the co-cultured strains reached a progressively stable ratio upon long-term continuous cultivation, even without control (Figure 1F; co-culture tended to equal abundance until the end of the experiment) or was reached even more quickly upon applying the AAMN approach (Figure 1D). As stated earlier, while LAB-KAZ exhibits a stabilizing effect through mutual cross-feeding, ECO-SAC does not share this benefit. This behavior was clearly observed during continuous cultivation (Figure 1G) and also upon applying AAMN (Figure 1E), where microbial species tended to escape AAMN control because they had the metabolic capability to contend for all MNs. Competitivity and cooperativity behavior can be more easily observed based on the error measurement recorded for the AAMN control (Note S5 in the supplemental information online).

To understand what drives either competitive or cooperative behavior, we considered **elementary mode (EM)** analysis of the central metabolism derived from existing genome-scale and other metabolic models for the different species involved (Figure 2A,B and Notes S1 and S2 in the supplemental information online) to quantitatively characterize the stoichiometric degree of competitivity (θ) between strains (Figure 2C). θ depends on the MNs available for the growth of each species. For example, if a substrate can be used by both species in the co-culture, it will lead to high competitivity and, accordingly, a θ value close or equal to 1. By contrast, if another substrate can be used by only one of the species, this will lead to the appearance of an exclusive MN promoting the growth of this species only, ultimately leading to a reduction in θ. We applied this approach to the analysis of the MNs that were expected during the continuous cultivation experiments [19,23,38]. In an ideal case, we could exploit totally exclusive niches ($\theta = 0$) for each strain and alternate between them at a given rhythm adjusted to the desired mean growth rates. In reality, MNs commonly overlap, increasing the competitivity and reducing the stability of the system because the faster consumer will eventually overtake each niche over time [21,39].

We determined the most relevant metabolic pathways for each species in co-culture pairs based on genome-scale metabolic network and EM analysis (Figure 2A,B and Note S2). Based on this approach, we determined the metabolic space for each microbe resulting from the metabolic flux distributions with the major substrate consumption capabilities used for biomass generation based on byproducts utilization (Figure 2B). The results were displayed in a yield convex solution space for three different potential substrates (Figure 2B), where each dot represents an EM and its position the biomass yield ($Y_{x/s}$) for any specific substrate. The most extreme EM positions for each substrate can be selected to construct a polygon (NP) that contains all the MNs that can be used by each strain. The MN preference for each strain can be easily visualized based on the vertices of the NPs and can be used for computing the competitive advantage for each of the strains in the co-culture (Figure 2C). These NPs are multidimensional and contain the total capabilities of a strain. However, they can also be simplified to a selected active set of metabolic pathways, resulting from only accounting for the solutions concerning the existing environmental substrates where the microbial species are being cultured (Figure 3A,B for ECO–SAC and Note S2) [10,19].

Along with the active set of metabolic pathways, there are other minor pathways that could generate potential substrates. However, since the corresponding metabolites are not present in measurable concentrations in our cultivation conditions, these elements were neglected for the definition of the MNs. For better visualization, in the case of LAB-KAZ, two different NPs were constructed (i.e., one for the main carbon sources, and the other for the amino acids; Note S2). For the carbon source, the analysis of MN highlighted a clear overlap between LAB

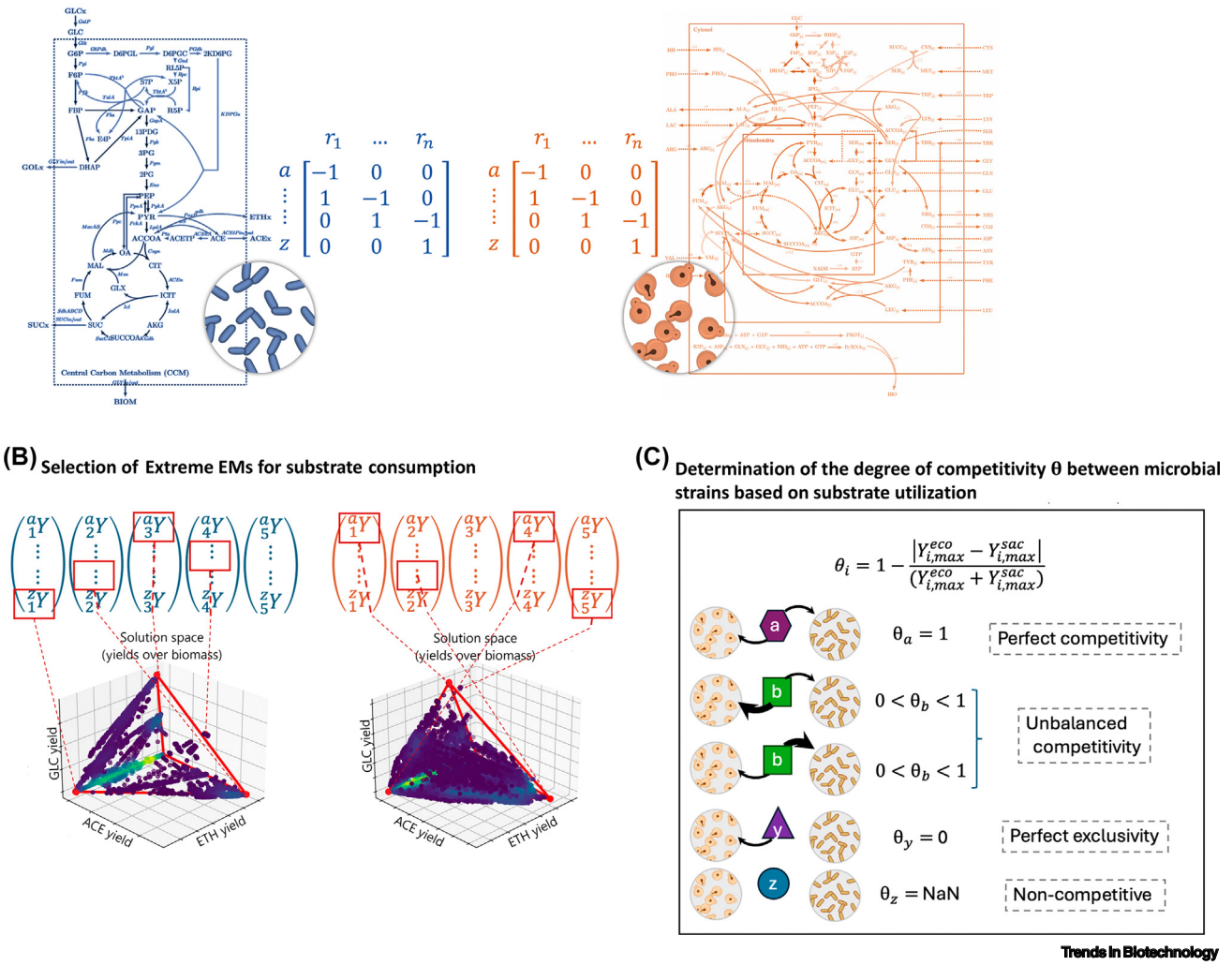

Figure 2. Framework for computing competitivity between strains involved in co-cultures. (A) Genome-scale models for *Escherichia coli (ECO) and Saccharomyces cerevisiae (SAC)* are processed to generate a stoichiometric matrix for each species. (B) Elementary mode (EM) analysis is performed on each stoichiometric matrix to identify the major pathways involved in biomass generation. Yield coefficients (i.e., Y_i) are then computed for each species and available substrates. (C) For each metabolite/substrate available in the extracellular medium, the degree of competitivity θ between strains can be computed based on the respective Y_i. Different scenarios from perfect competitivity (both cells consuming the substrate at an equal rate) to perfect exclusivity (monopolization of a substrate) and to noncompetitive (non-used substrate) are shown. Abbreviations: ACE, acetate; ETH, ethanol.

and KAZ. However, in this case, competitive exclusion can be avoided based on maltose feeding and glucose pulsing during the AAMN experiment and the resulting glucose cross-feeding. For the amino acid, the NP revealed that KAZ produced glycine and isoleucine that entered a cross-feeding metabolic flux with LAB, relieving its auxotrophy. In the case of KAZ-LAB, there was an increased degree of cooperation due to the auxotrophies from LAB and the KAZ substrate inaccessibility, which increased the stability of the co-culture, even in the face of the glucose metabolic overlap that can be observed based on the NPs. In other words, the temporal generation of suitable MNs for each species is ensured by the mutual cross-feeding provided by the amino acids naturally released by the yeast and the maltose pulsed during continuous cultivation. As a result, the AAMN leads to lower noise and disturbances in the control of the co-culture composition over time (Figure 1F).

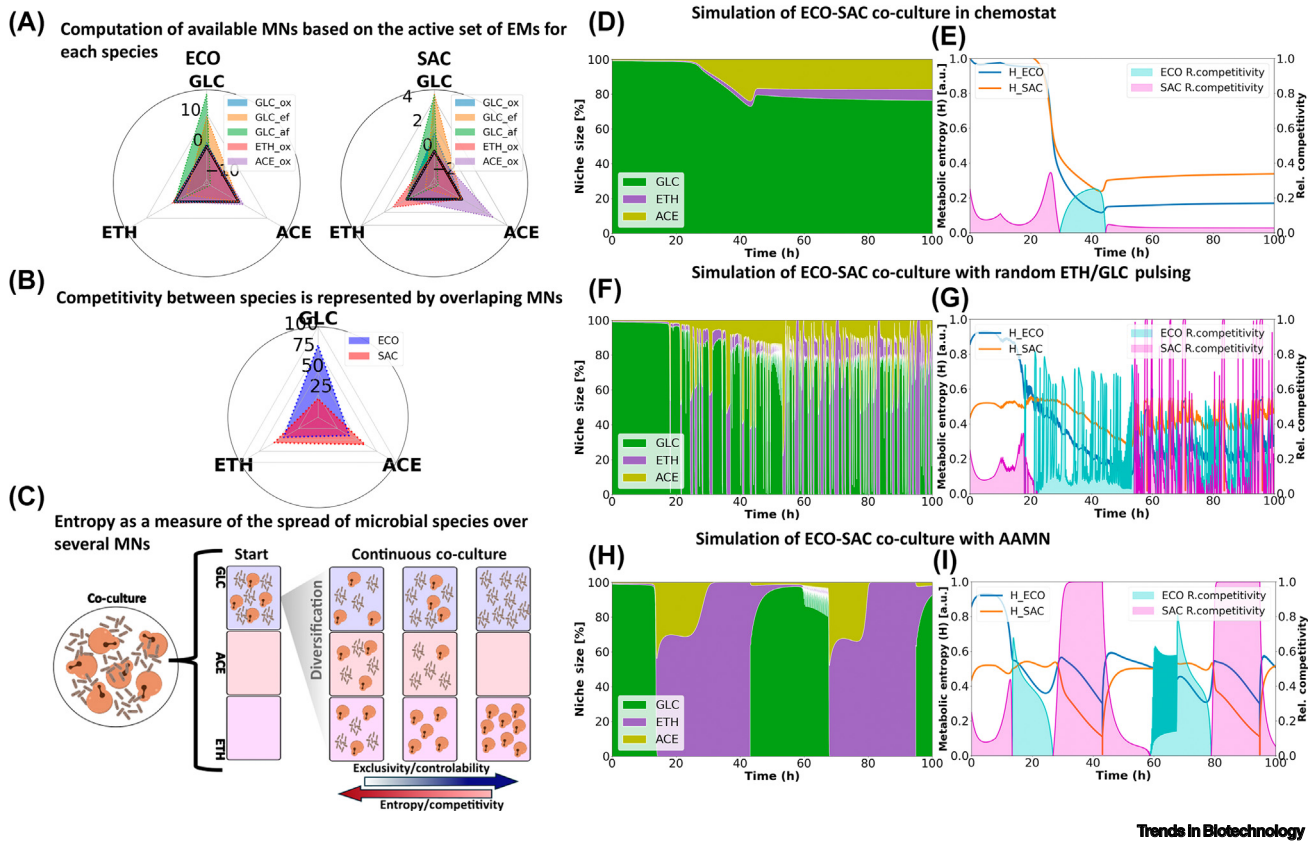

Figure 3. Full reversion of metabolic niches (MNs) is needed for stabilizing competitive *Escherichia coli* (ECO)-*Saccharomyces cerevisiae* (SAC) co-cultures. (A) Metabolic niche polygon representing the utilization of various substrate by the co-cultured species (i.e., ECO and SAC). These niche polygons were computed based on the biomass yields $Y_{x/s}$ obtained from the metabolic pathways contributing the most to growth based on elementary mode (EM) analysis. (B) Overlap between two niche polygons can be used for estimating the stoichiometric degree of competitivity between two microbial species, since the corresponding MNs are not exclusive in case of overlap. (C) Relative competitivity based on growth and Information entropy can be used for estimating the dynamic dispersion of one species to the mobilization of several MNs. When the computation is performed for two species, the comparative analysis of the partial entropies can be used for determining either controllability based on the exclusivity of the MNs, or the degree of competition between species. (D) Simulation of the evolution of the MN size for the ECO-SAC co-culture growing in a chemostat. (E) Evolution of the relative competitivity and entropy computed from the comparative MN repartition between ECO and SAC in a chemostat. (F) Simulation of the evolution of the MN size for the ECO-SAC co-culture in continuous mode with random substrate [ethanol (ETH) and glucose (GLC)] pulsing. (G) Evolution of the relative competitivity and entropy computed from the comparative MN repartition between ECO and SAC in a continuous cultivation device with random ETH/GLC pulsing. (H) Simulation of the evolution of the MN size for the ECO-SAC co-culture in continuous mode where ETH and GLC are pulsed according to automated adjustment of metabolic niches (AAMN). (I) Evolution of the relative competitivity and entropy computed from the comparative MN repartition between ECO and SAC in a continuous cultivation device with ETH/GLC pulsing performed based on AAMN. Abbreviation: ACE, acetate.

For ECO-SAC, the NP revealed that the MNs for each species were all overlapping (Figure 3A,B), explaining the competitive behavior observed during the experiments (Figure 3C). In this case, this overlap was not compensated for by cross-feeding. Indeed, even if overflow metabolites (ACE and ETH) were released, they were not mutually exclusive for one of the species, further contributing to the system destabilization because bacteria and yeast growth rates are significantly different in all metabolites.

To compute the stability of the co-cultures, we could use θ; however, this computes the competitivity of the strains in fair (i.e., same masses) and stationary conditions only. Thus, we established a quantitative approach for determining the competitivity dynamics between microbes based on the actual growth rate of the species in co-culture. Furthermore, we compared this relative competitivity to parameters derived from the computation of information

entropy (H) (i.e., Shannon's entropy; Note S4 in the supplemental information online). The concept of information entropy is frequently used for computing the degree of phenotypic heterogeneity of monocultures based on the distribution of the phenotype [28,40,41]. We used a similar approach to capture the spread of the microbial species over the utilization of several MNs (Figure 3C). Based on the computation of the respective entropies related to the dispersion of one species over several potential MNs, it was then possible to derive parameters about the degree of cooperativity/competitivity between species (Notes S2–S4 in the supplemental information online). This information entropy calculation is based on the estimation of the probability of finding cells consuming a substrate based on the simulated instantaneous individual consumption rates, therefore providing a more dynamic view of the competition and instantaneous niche colonization rather than the previously formulated θ, which compares only the maximum metabolic capabilities.

Furthermore, measuring the partial entropy exhibited by each strain in the co-culture allowed us to determine how well the substrates were distributed along the strains, and therefore, the exclusivity of substrate utilization (Note S4). In addition, this dynamic approach enabled us to calculate how efficient pulses or perturbations would change the systems composition (i.e., its controllability). We then used these proxies in different co-culture scenarios (Figure 3D–I).

It has been observed that AAMN is important in the case of ECO-SAC co-cultures for continuously adjusting the MNs during co-culture. Thus, the precise adjustment of the MN based on substrate pulsing appears vital for stabilizing competitive co-cultures. To challenge this hypothesis, we conducted dynamic simulation of ECO-SAC co-cultures based on different cultivation scenarios [i.e., chemostat (Figure 3D,E), random pulsing cultivation (Figure 3F,G), or AAMN (Figure 3H,I)]. For this purpose, we used a previously developed dynamic modeling toolbox, called MONCKS [13], complemented with the main metabolic pathways identified based on EM analysis (a brief description of the simulation protocols and equations used for the models is provided in Note S3 in the supplemental information online). As expected, the dynamic simulations pointed out stabilization in the case of cultivation conducted under AAMN, whereas population collapse was observed in the case of chemostat or random pulsing cultivation (this latter scenario was further validated experimentally; Note S3). These results point out that, even if the NPs reveal strong niche overlap, AAMN can be used for reverting the MNs at a specific frequency, leading to the stabilization of the co-culture [10] (Figure 3G,H).

Engineering cooperativity in continuous co-cultures of ECO and SAC

Whereas the AAMN approach can be used for stabilizing co-cultures exhibiting competitive behavior, the results pointed out a population oscillatory profile (Figure 1E), which might not be convenient to exploit for applications such as bioproduction, where a more stable co-culture profile is expected [42]. Thus, we implemented a separation of carbon sources in an attempt to promote cooperative behavior between ECO and SAC [6,7,43]. To do so, we used an ECO strain defective in active glucose transport [44,45], and the alternative pulsing of glucose and xylose to generate MNs promoting the growth of SAC (SAC*) and ECO (ECO*), respectively. We then adapted the metabolic fluxes for these strains and recomputed θ. As expected, θ decreased, and the controllability of the system increased from 9.1% to 28.3% (Note S2). The ECO* strain exhibited deletion of components of phosphotransferase system (PTS)-dependent sugar transporters, as well as non-PTS-transporters [44,45]. As a result, this strain exhibited reduced glucose uptake and ACE excretion, allowing the yeast to grow mainly on glucose during co-cultivation. Xylose was considered a second carbon source for ensuring the coexistence of the ECO* strain. This separation of carbon source is expected to provide more control over co-culture composition [6,7,42]. We adapted the metabolic fluxes accordingly and performed the EM analysis to define the NP for the two microbial species (Figure 4A). These computations were complemented by dynamic simulations of the ECO*-SAC* co-culture based on MONCKS (Figure 4B–D and Note S3).

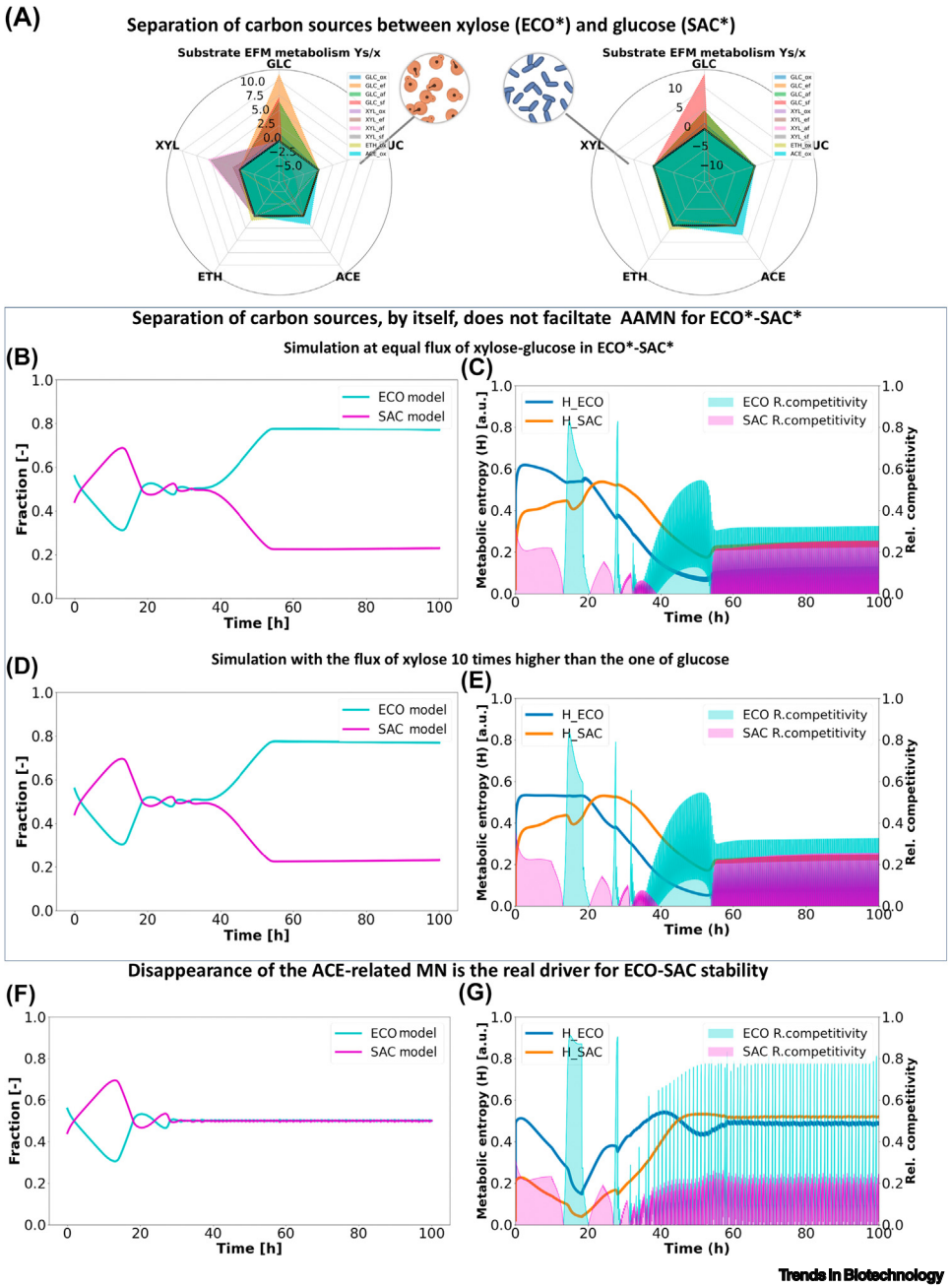

Figure 4. Elementary mode (EM) analysis and Monod-type co-culture kinetic simulation (MONCKS) predict that the suppression of the acetate (ACE)-related metabolic niche (MN) promotes cooperativity in *Escherichia coli* (ECO)-*Saccharomyces cerevisiae* (SAC) co-cultures. (A) MNs for ECO* and SAC* computed from EM analysis of genome-scale metabolic models. The values represent the biomass yield $Y_{x/s}$ for the different EMs, corresponding here to the different MNs. (B) Dynamic simulation based on MONCKS and showing the evolution of the fraction of ECO* and SAC* in automated adjustment of metabolic niches (AAMN) continuous cultures at a dilution rate D = 0.1 h^{-1} with controlled additions of glucose (GLC) and xylose (XYL; 0.4 g per pulse) and GLC and XYL ECO maximum consumption rates with equal values. (C) Evolution of the relative competitivity and entropy of the in AAMN continuous co-culture operated with an equal feed of GLC and XYL maximum consumption rates. (D) Dynamic simulation based on MONCKS and showing the evolution of the fraction of ECO* and SAC* in AAMN continuous cultures at a dilution rate D =

(Figure legend continued at the bottom of the next page.)

We first conducted the simulations by adjusting the uptake rate of glucose and xylose by ECO*-SAC*. In the first simulation, we considered that the rate of glucose uptake and xylose was equivalent. While this computation should lead to the 50:50 control setpoint for the ECO*-SAC co-culture, simulation pointed out that the populations escape AAMN control and stabilize far from the set point after ~40 h of cultivation (Figure 4B). Interestingly, this destabilizing effect was independent of the glucose–xylose uptake rate ratio (Figure 4D). Furthermore, the relative competitivity oscillated between the organisms, leading to stabilization. The calculated partial entropies of both microorganisms were low, indicating a monopolization (i.e., exclusive use of a substrate by a single species) of substrates (Figure 4C,E). Analysis of niche size then showed that the escape from control was the result of the appearance of an unexpected and uncontrolled MN involving ACE. Indeed, ACE is produced by ECO upon overflow metabolism and can be reassimilated by both species upon adaptation in continuous cultures, leading to new MNs contributing to the stabilization of the co-culture far from the control setpoint (Figure 4C,E and Notes S3 and S4). Oscillations were observed due to cycles of production and consumption of ACE. The ECO* strain is defective in the PTS and is unable to produce ACE due to its reduced glucose consumption rates [44,45]. However, it is capable of ACE production if the pyruvate and phosphoenolpyruvate nodes are saturated, arising from glucose and xylose co-utilization.

We then studied the possibility of minimizing the MN related to ACE by reducing the EM ACE yield in the models and reprocessed dynamic simulation based on MONCKS (Figure 4F), which, this time, predicted co-culture stabilization at the 50:50 setpoint based on AAMN. In this case, the ACE niche never reached a large enough size to impact the relative competitivity of the strains and, therefore, the oscillations at the stabilization time were mostly made by the oscillating pulses given by the AAMN actuator (i.e., in our case the pump providing xylose or glucose pulsing). This result is important because it highlights that the simple separation of carbon sources is not necessarily an effective approach for stabilizing co-culture if cross-feeding and other unexpected niches are not considered for the control strategy. In some cases, such as that considered here, consumption of alternative carbon source can lead to the emergence of unwanted MNs, moving the stabilizing condition of the co-culture further from a control setpoint designed in the AAMN. More generally, these results point out that our simulation toolbox could be generalized for probing different metabolic engineering strategies aiming at stabilizing co-culture. Next, we challenged experimentally the utilization of the ECO*-SAC* co-culture for the continuous bioproduction of p-coumaric acid.

AAMN is effective for promoting division of labor and coumaric acid production by ECO*-SAC* co-culture

One of the key benefits of using co-cultures instead of monocultures is their ability to enhance the metabolic capabilities of the system, based on the division-of-labor principle [6,20,43,46]. Accordingly, we adapted our potentially cooperative ECO*-SAC* co-culture (Figure 4D) for the continuous bioproduction of p-coumaric acid. ECO* and SAC* were then further engineered to produce tyrosine and its bioconversion to p-coumaric acid (Figure 5A). ECO* was engineered for tyrosine overproduction, while SAC* was engineered for converting excess tyrosine to p-coumaric acid.

0.1 h^{-1} with controlled additions of GLC and XYL (0.4 g per pulse), GLC ECO maximum consumption rates were ten times lower than those for XYL. (E) Evolution of the relative competitivity and entropy of the AAMN continuous co-culture operated with XYL rates ten times higher than those of GLC. (F) Dynamic simulation based on MONCKS and showing the evolution of the fraction of ECO* and SAC* in AAMN continuous cultures at a dilution rate D = 0.1 h^{-1} with controlled additions of GLC and XYL (0.4 g per pulse), with ACE and ethanol (ETH) production yields ten times lower than XYL maximum consumption rates. (G) Evolution of the relative competitivity and entropy of the AAMN continuous co-culture operated in reduced ACE and ETH overflow metabolism conditions.

We first carried out chemostat experiments in which different xylose:glucose ratios were considered as co-feeding (Figure 5B). Upon reducing the amount of xylose in the feed, stabilization of the co-culture naturally occurred after 60 h of cultivation, without the need for AAMN. This observation

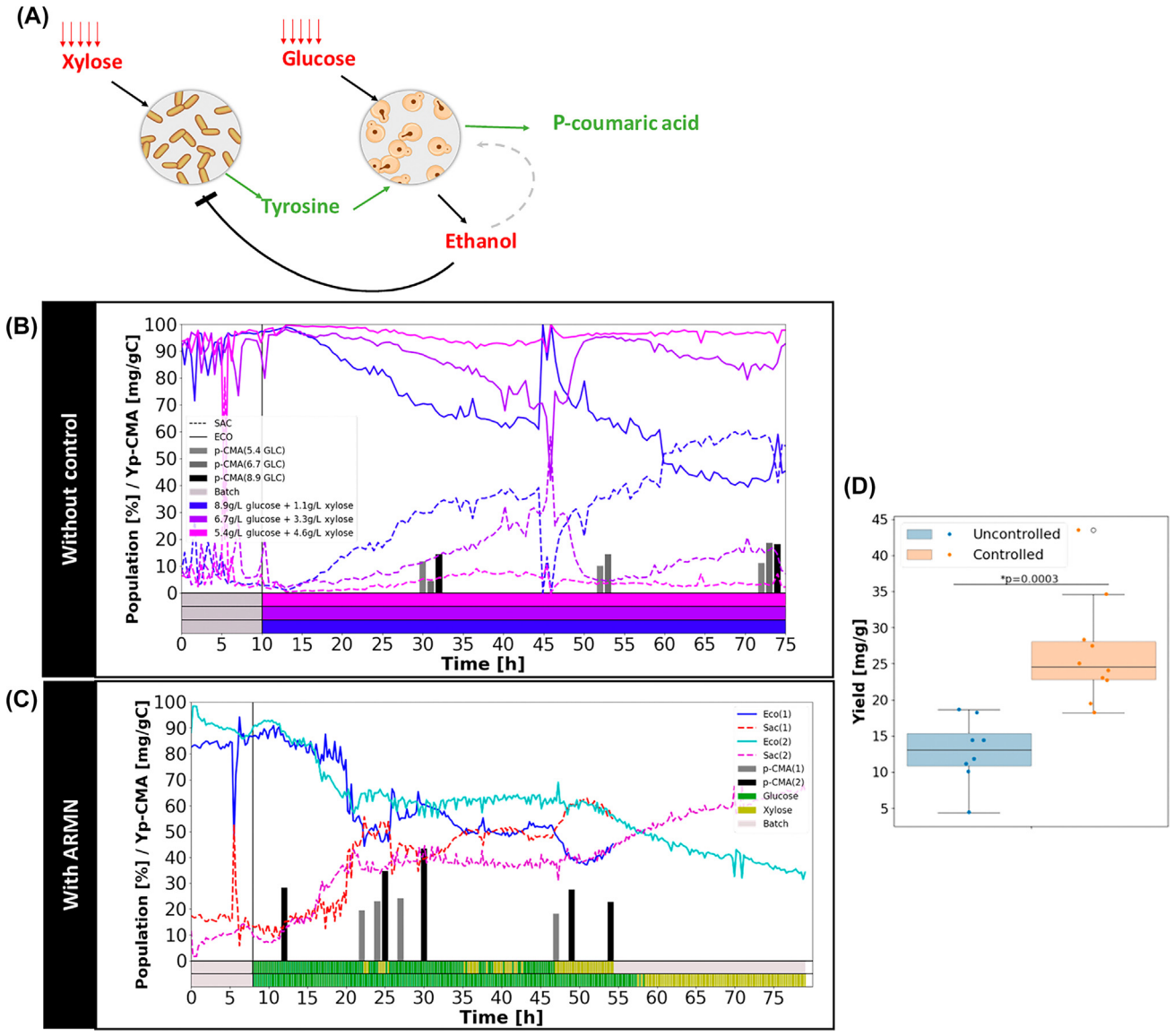

Figure 5. Automated adjustment of metabolic niches (AAMN) allows for stabilization of *Escherichia coli (ECO*)-Saccharomyces cerevisiae (SAC*)* co-culture engineered to produce p-coumaric acid. (A) Schematic of the metabolic interactions occurring in the context of the ECO*-SAC* co-culture. (B) Evolution of the number of cells (as determined based on automated flow cytometry; FC) for the ECO*-SAC* co-cultures in a chemostat with variable xylose (XYL)/glucose (GLC) feeding ratios. (C) Evolution of the number of cells (as determined based on automated FC) for an ECO*-SAC* co-culture in a continuous cultivation device with AAMN in duplicate (nutrient pulsing profile at the bottom of the figure). (D) Comparison of para-coumaric acid (p-CA) to substrate yields (g p/C g of GLC + C g of XYL) between continuous cultures performed with and without AAMN. Yields were calculated from samples from all experiments after 24 h; all samples from the AAMN were clustered to make the controlled type box plot (sample size = 10) and compared with all uncontrolled samples boxplot (sample size = 8); an ANOVA single tail test was performed and revealed a significant difference between the populations with $P \leq 0.0003$. Abbreviations: ACE, acetate; ETH, ethanol; Y p-CMA, yield in para-coumaric acid in mg/g of carbon consumed. The red arrows indicate whether substrate is added by pulses or continuously during the cultivation.

confirmed that the separation of carbon sources promoted cooperative behavior in ECO*-SAC* co-cultures. We then considered AAMN for enhancing the stabilization of the co-cultures (Figure 5C). Upon AAMN, partial stabilization of the co-cultures was observed readily after ~20 h of cultivation. However, the cooperative behavior of ECO*-SAC* was not as elevated as that reported for LAB-KAZ (Figure 1D) or that predicted by MONCKS (Figure 4D). By contrast, AAMN allowed for the stabilization of the ECO*-SAC* co-culture, resulting in a 3.5-fold improvement in p-coumaric acid yield over carbon (gC from glucose + gC from xylose) compared with chemostat cultures (Figure 5D).

Several explanations can be advanced at this level. First, the toxicity of the product (i.e., p-coumaric acid) can impact the stability of the co-cultures. Second, the theoretical destabilization found with MONCKS in the previous section, by the apparition of unwanted or uncontrolled MN such as ACE or ETH, could impair AAMN. Third, cellular co- and/or auto-aggregation was observed based on automated FC profiles (Note S5). Aggregation directly impacts co-culture stability since it has been previously reported that cell auto- or co-aggregation can lead to collective elimination in some ecosystems [47]. In addition, auto-aggregation of yeast cells was previously reported to decrease the performance of bioethanol production upon bacterial contamination [48]. Finally, aggregation also introduces error into the estimation of events and, therefore, in the AAMN actuator performance. However, the FC data did not highlight out any difference in the intensity of cell aggregation between the different co-cultures (i.e., either cooperative and competitive), suggesting product toxicity and/or uncontrolled MNs as the main drivers for co-culture destabilization in the case of ECO*-SAC*. Even with the increase found in p-coumaric acid concentration, this process is still far from the theoretical maximum, as these strains have not been fully optimized for tyrosine and p-coumaric acid production. However, we established as a proof of concept the control of co-culture in a continuous cultivation device to produce metabolites based on a division-of-labor approach.

Discussion

Cell–machine interfaces, relying either on microfluidics [49,50] or FC [28,51], can be used for manipulating gene expression in individual cells within a population, leading to the acquisition of data for characterizing gene circuits [50,52] or, from a more applied perspective, to improved bioproduction [29,53,54]. Similar approaches were recently applied for manipulating co-culture composition over time [14,15]. However, most of these approaches rely on the use of synthetic genetic circuits for establishing stable co-cultures, while, in this work, we exploited the natural capabilities and dynamics of strains to explore the environment and diversify into different MNs. Therefore, we propose a generalizable approach, relying only on the use of nutrient pulsing, for adjusting the MNs and strain coexistence. Based on our AAMN approach, we were able to control three different types of yeast–bacteria co-culture, including the ones exhibiting strong competitive behavior. Synthetic biology provides numerous different technologies aiming at controlling co-cultures and/or microbial communities [25,55,56]. However, most of the technologies proposed so far come at a high metabolic load for the hosts [57,58] or with harsh consequences for the targeted species (e.g., cell lysis) [59]. As an example, systems involving either toxin–antitoxin or bacteriocins appear effective [60], but results in cell lysis for controlling the dominance of one of the species. For applications such as bioprocessing, cell death and lysis must be avoided, since they can lead to loss of resources and productivity, as well as issues related to downstream processing operations. Unwanted cell lysis can be prevented based on the use of other technologies, such as quorum sensing circuits, for controlling the cell density of the different species [61–64]. However, the signaling molecules used for probing and controlling cell density (e.g., acyl-homoserine lactones) can be diluted upon scaling-up, further impairing the transposition of the system to industrial applications.

It is also possible to dynamically control gene circuits based on light (optogenetics) [51,53], and this technology has already been used to control gene circuits for the stabilization of co-cultures [14]. Again, the utilization of light as an actuator for cell population control is difficult to scale up, due notably to the limit of transmission of light and large, dense cell suspension volumes [65]. Here, we showed that nondestructive strategies, such as the separation of carbon sources, and AAMN, can be used for promoting cooperative behavior in ECO-SAC co-cultures. We also revealed that timing in the adjustment of the MNs is critical for stabilizing the co-culture composition. Accordingly, such an approach requires the precise quantification of the related MNs. It is now possible to define more precisely the MNs based on the utilization of genome-scale metabolic models [18–21,23]. We carried out EM analysis based on the metabolic networks of the six naturally engineered species considered in this study. Surprisingly, we find out that only a limited set of EMs (i.e., between three and five) were needed for recapitulating co-cultures dynamics (except in the specific case of amino acid exchange for LAB-KAZ, where more than 20 EMs were involved) based on the use of the MONCKS toolbox [13].

While the AAMN approach can be effective in analyzing population dynamics, it does have a limitation in terms of noise in control efficiency, particularly when considering competitive co-cultures, such as ECO-SAC. This is likely due to the simplicity of the pulse ON/pulse OFF controller, which can lead to overshoots. To overcome this limitation, future improvements to the controller could be explored. Nevertheless, the AAMN approach is valuable to analyze the population dynamics in response to the availability of MNs and their expansion/contraction upon metabolic diversification of the microbial species being studied. This can provide valuable insights into the dynamics of microbial communities and inform strategies for optimizing their behavior. Taken altogether, the experimental and numerical tools developed in this work can be used as a general approach for capturing microbial co-culture dynamics and enabling the development of applications, such as continuous bioprocesses.

Concluding remarks

Developing new techniques and protocols to understand how species coexist and identify the ecological drivers of this coexistence is essential for unlocking the potential of microbial communities in bioprocessing. The Segregostat approach, coupled with the AAMN protocol, addresses this phenomenon while offering the added benefit of enabling enhanced process controllability without the need to modify strains. This increases the flexibility for engineering desired metabolic capabilities tailored for the production purposes. Moreover, AAMN not only advances bioprocess engineering, but also, in combination with dynamic metabolic models, offers valuable insights into metabolic interactions, mass and energy fluxes, and the relationships between organisms in microbial communities. This understanding is crucial for broader biological disciplines, such as systems ecology.

The Segregostat-AAMN protocol, as presented, still holds significant potential for further optimization. Opportunities to increase its control effectiveness include the integration of model predictive controllers or artificial intelligence (AI)-based approaches, and the incorporation of more complex actuators, such as support for pulsing multiple metabolites at varying rates and frequencies. In addition, incorporating process parameters, such as pH, temperature, and oxygen transfer, could further enhance the approach robustness in terms of control for multiple organisms. Furthermore, the approach could be strengthened by adopting novel high-throughput population measurement techniques beyond flow cytometry. This could improve modeling accuracy and refine our understanding of complex phenomena, such as phenotype diversification, metabolic cooperation, and broader community behaviors (see Outstanding questions). By contrast, in its current developmental state, the approach is simple to implement and basing it

Outstanding questions

Can the competitive exclusion principle be exploited for understanding and stabilizing microbial communities in a continuous cultivation device?

Is full cybernetic metabolic flux analysis able to provide dynamic insight into the possible novel MNs that could be exploited by a microbial community?

What is the range of frequencies of alternation between MNs promoting the coexistence of two or more different organisms in the same cultivation device?

Is it possible to model or predict by AI the pattern of alternance between two or more MNs for better stabilizing control of co-cultures?

Can this approach be scaled-up for enabling continuous bioprocessing?

on such broad microbial characteristics, such as MN competition and diversification, should make it easy to use robustly in a range of studies of applications. Thus, we believe that the approach presented here represents a significant contribution toward realizing the long-desired goal of harnessing microbial communities for numerous bioprocessing technologies.

STAR★METHODS

Detailed methods are provided in the online version of this paper and include the following:

- KEY RESOURCES TABLE
- EXPERIMENTAL MODEL AND STUDY PARTICIPANT DETAILS
  - Bacterial strains
  - Yeast strains
- METHOD DETAILS
  - Chemostat and Segregostat cultivations
  - Central carbon metabolic network model construction
  - Elementary mode (EM) analysis
  - Dynamic metabolic flux modeling
  - Competitivity and controllability analysis
- QUANTIFICATION AND STATISTICAL ANALYSIS
  - FC data treatment
  - Metabolite analysis

RESOURCE AVAILABILITY

Lead contact

Further information and requests for resources and materials should be directed to, and will be fulfilled if possible by, the lead contact, Frank Delvigne (f.delvigne@uliege.be).

Materials availability

This study did not generate new unique reagents.

Data and code availability

The raw data sets are available on GitLab (https://gitlab.uliege.be/mipi/published-software/2024-cocultures). Extra data, tables, graphs, and documentation can be found in the supplemental information online as a single file. An updated version of MONCKS within the full MiPI Biomass Modelling and Simulation toolbox (BMS in mBioMAS) and the full MiPI Flow Cytometry Analysis toolbox (FCA in mBioMAS) are provided on GitLab (https://gitlab.uliege.be/mipi/published-software/mbiomas-core).

Author contributions

J.A.M. performed the experiments related to ECO-SAC co-culture, developed the computational toolbox, and drafted the manuscript. R.B. performed the experiments related to LAB-KAZ and ECO*-SAC*. T.G.S.A. performed the experiments related ECO*-SAC* to produce p-coumaric acid. G.G. designed the strains involved in ECO*-SAC*. L.M.M. and L.C. constructed the ECO*-SAC* strains. F.D. captured grants and funding, developed the concept of MNs, supervised the research, and wrote the manuscript.

Acknowledgments

J.A.M. is supported by a postdoctoral grant provided by the Service Public de Wallonie (SPW) and the H2020 program of the European Commission (Era-Cobiotech project Contibio). R.B. is supported by a postdoctoral grant provided by the SPW for the Sunup project. T.G.S.A. is supported by a PhD grant provided by the 'Fonds de la Recherche Scientifique' FRS-FNRS, from the Walloon region of Belgium. F.D. received funding from a research grant provided by the SPW and the H2020 program of the European Commission (Era-Cobiotech project Contibio). The participation of Caheri Salas in the construction of the yeast p-coumaric acid production strain is acknowledged. We would also like to acknowledge Laurie Josselin for her helping reviewing the manuscript.

Declaration of interests

The authors declare no competing interests.

Supplemental information

Supplemental information to this article can be found online at https://doi.org/10.1016/j.tibtech.2024.12.005.

References

1. Hu, J. *et al.* (2022) Emergent phases of ecological diversity and dynamics mapped in microcosms. *Science* 378, 85–89
2. Oña, L. *et al.* (2021) Obligate cross-feeding expands the metabolic niche of bacteria. *Nat. Ecol. Evol.* 5, 1224–1232
3. Ratzke, C. *et al.* (2020) Strength of species interactions determines biodiversity and stability in microbial communities. *Nat. Ecol. Evol.* 4, 376–383
4. Goldford, J.E. *et al.* (2018) Emergent simplicity in microbial community assembly. *Science* 361, 469–474
5. Aulakh, S.K. *et al.* (2023) Spontaneously established syntrophic yeast communities improve bioproduction. *Nat. Chem. Biol.* 19, 951–961
6. Zhou, K. *et al.* (2015) Distributing a metabolic pathway among a microbial consortium enhances production of natural products. *Nat. Biotechnol.* 33, 377–383
7. Jiang, Y. *et al.* (2023) Construction of stable microbial consortia for effective biochemical synthesis. *Trends Biotechnol.* 41, 1430–1441
8. Blox Bloxham *et al.* (2024) Biodiversity is enhanced by sequential resource utilization and environmental fluctuations via emergent temporal niches. *PLoS Comput. Biol.* 20, e1012049
9. Colwell, R.K. and Rangel, T.F. (2009) Hutchinson's duality: the once and future niche. *Proc. Natl. Acad. Sci. U. S. A.* 106, 19651–19658
10. Malard, L.A. and Guisan, A. (2023) Into the microbial niche. *Trends Ecol. Evol.* 38, 936–945
11. Mancuso, C.P. *et al.* (2021) Environmental fluctuations reshape an unexpected diversity-disturbance relationship in a microbial community. *eLife* 10, e67175
12. Rodríguez-Verdugo, A. *et al.* (2019) The rate of environmental fluctuations shapes ecological dynamics in a two-species microbial system. *Ecol. Lett.* 22, 838–846
13. Martinez, J.A. *et al.* (2022) Controlling microbial co-culture based on substrate pulsing can lead to stability through differential fitness advantages. *PLoS Comput. Biol.* 18, e1010674
14. Gutiérrez Mena, J. *et al.* (2022) Dynamic cybergenetic control of bacterial co-culture composition via optogenetic feedback. *Nat. Commun.* 13, 4808
15. Salzano, D. *et al.* (2022) Ratiometric control of cell phenotypes in monostrain microbial consortia. *J. R. Soc. Interface* 19, 20220335
16. Dolinšek, J. *et al.* (2016) Synthetic microbial ecology and the dynamic interplay between microbial genotypes. *FEMS Microbiol. Rev.* 40, 961–979
17. Schäfer, M. *et al.* (2023) Metabolic interaction models recapitulate leaf microbiota ecology. *Science* 381, eadf5121
18. Fahimipour, A.K. and Gross, T. (2020) Mapping the bacterial metabolic niche space. *Nat. Commun.* 11, 4887
19. Régimbeau, A. *et al.* (2022) Contribution of genome-scale metabolic modelling to niche theory. *Ecol. Lett.* 25, 1352–1364
20. Shahab, R.L. *et al.* (2020) Engineering of ecological niches to create stable artificial consortia for complex biotransformations. *Curr. Opin. Biotechnol.* 62, 129–136
21. van den Berg, N.I. *et al.* (2022) Ecological modelling approaches for predicting emergent properties in microbial communities. *Nat. Ecol. Evol.* 6, 855–865
22. Shepherd, E.S. *et al.* (2018) An exclusive metabolic niche enables strain engraftment in the gut microbiota. *Nature* 557, 434–438
23. Noecker, C. *et al.* (2023) Systems biology elucidates the distinctive metabolic niche filled by the human gut microbe *Eggerthella lenta*. *PLoS Biol.* 21, e3002125
24. Rodriguez, A. *et al.* (2015) Establishment of a yeast platform strain for production of p-coumaric acid through metabolic engineering of aromatic amino acid biosynthesis. *Metab. Eng.* 31, 181–188
25. Ronda, C. and Wang, H.H. (2022) Engineering temporal dynamics in microbial communities. *Curr. Opin. Microbiol.* 65, 47–55
26. Ryo, M. *et al.* (2019) Basic principles of temporal dynamics. *Trends Ecol. Evol.* 34, 723–733
27. Delvigne, F. and Martinez, J.A. (2023) Advances in automated and reactive flow cytometry for synthetic biotechnology. *Curr. Opin. Biotechnol.* 83, 102974
28. Henrion, L. *et al.* (2023) Fitness cost associated with cell phenotypic switching drives population diversification dynamics and controllability. *Nat. Commun.* 14, 6128
29. Nguyen, T.M. *et al.* (2021) Reducing phenotypic instabilities of a microbial population during continuous cultivation based on cell switching dynamics. *Biotechnol. Bioeng.* 118, 3847–3859
30. Boudaoud, S. *et al.* (2021) Sourdough yeast-bacteria interactions can change ferulic acid metabolism during fermentation. *Food Microbiol.* 98, 103790
31. Gabrielli, N. *et al.* (2023) Unravelling metabolic cross-feeding in a yeast-bacteria community using (13) C-based proteomics. *Mol. Syst. Biol.* 19, e11501
32. Ponomarova, O. *et al.* (2017) Yeast creates a niche for symbiotic lactic acid bacteria through nitrogen overflow. *Cell Syst.* 5, 345–357
33. Stolz, P. *et al.* (1993) Utilisation of maltose and glucose by lactobacilli isolated from sourdough. *FEMS Microbiol. Lett.* 109, 237–242
34. Carbonetto, B. *et al.* (2020) Interactions between *Kazachstania humilis* yeast species and lactic acid bacteria in sourdough. *Microorganisms* 8, 240
35. Losoi, P.S. *et al.* (2019) Enhanced population control in a synthetic bacterial consortium by interconnected carbon cross-feeding. *ACS Synth. Biol.* 8, 2642–2650
36. Bull, J.J. and Harcombe, W.R. (2009) Population dynamics constrain the cooperative evolution of cross-feeding. *PLoS ONE* 4, e4115
37. Kerner, A. *et al.* (2012) A programmable *Escherichia coli* consortium via tunable symbiosis. *PLoS ONE* 7, e34032
38. diCenzo, G.C. *et al.* (2016) Metabolic modelling reveals the specialization of secondary replicons for niche adaptation in *Sinorhizobium meliloti*. *Nat. Commun.* 7, 12219
39. Machado, D. *et al.* (2021) Polarization of microbial communities between competitive and cooperative metabolism. *Nat. Ecol. Evol.* 5, 195–203
40. Henrion, L. *et al.* (2022) Exploiting information and control theory for directing gene expression in cell populations. *Front. Microbiol.* 13, 869509
41. Hansen, A.S. and O'Shea, E.K. (2015) Limits on information transduction through amplitude and frequency regulation of transcription factor activity. *eLife* 4, e06559
42. McCarty, N.S. and Ledesma-Amaro, R. (2019) Synthetic biology tools to engineer microbial communities for biotechnology. *Trends Biotechnol.* 37, 181–197
43. Zhang, S. *et al.* (2018) Interkingdom microbial consortia mechanisms to guide biotechnological applications. *Microb. Biotechnol.* 11, 833–847
44. Fragoso-Jiménez, J.C. *et al.* (2019) Growth-dependent recombinant product formation kinetics can be reproduced through engineering of glucose transport and is prone to phenotypic heterogeneity. *Microb. Cell Factories* 18, 26
45. Fragoso-Jiménez, J.C. *et al.* (2022) Glucose consumption rate-dependent transcriptome profiling of *Escherichia coli* provides insight on performance as microbial factories. *Microb. Cell Factories* 21, 189
46. Hays, S.G. *et al.* (2015) Better together: engineering and application of microbial symbioses. *Curr. Opin. Biotechnol.* 36, 40–49
47. Kim, K. and You, L. (2020) Bacterial aggregation leads to collective elimination. *Trends Microbiol.* 28, 243–244
48. Carvalho-Netto, O.V. *et al.* (2015) *Saccharomyces cerevisiae* transcriptional reprograming due to bacterial contamination during industrial scale bioethanol production. *Microb. Cell Factories* 14, 13
49. Lugagne, J.-B. *et al.* (2017) Balancing a genetic toggle switch by real-time feedback control and periodic forcing. *Nat. Commun.* 8, 1671

50. Rullan, M. *et al.* (2018) An optogenetic platform for real-time, single-cell interrogation of stochastic transcriptional regulation. *Mol. Cell* 70, 745–756
51. Bertaux, F. *et al.* (2022) Enhancing bioreactor arrays for automated measurements and reactive control with ReacSight. *Nat. Commun.* 13, 3363
52. Lugagne, J.-B. and Dunlop, M.J. (2019) Cell-machine interfaces for characterizing gene regulatory network dynamics. *Curr. Opin. Syst. Biol.* 14, 1–8
53. Milias-Argeitis, A. *et al.* (2016) Automated optogenetic feedback control for precise and robust regulation of gene expression and cell growth. *Nat. Commun.* 7, 12546
54. Benisch, M. *et al.* (2023) Optogenetic closed-loop feedback control of the unfolded protein response optimizes protein production. *Metab. Eng.* 77, 32–40
55. Klitgord, N. and Segre, D. (2010) Environments that induce synthetic microbial ecosystems. *PLoS Comput. Biol.* 6, e1001002
56. Kong, W. *et al.* (2018) Designing microbial consortia with defined social interactions. *Nat. Chem. Biol.* 14, 821–829
57. Borkowski, O. *et al.* (2016) Overloaded and stressed: whole-cell considerations for bacterial synthetic biology. *Curr. Opin. Microbiol.* 33, 123–130
58. Ceroni, F. *et al.* (2018) Burden-driven feedback control of gene expression. *Nat. Methods* 15, 387–393
59. Din, M.O. *et al.* (2016) Synchronized cycles of bacterial lysis for in vivo delivery. *Nature* 536, 81–85
60. Liao, M.J. *et al.* (2019) Rock-paper-scissors: engineered population dynamics increase genetic stability. *Science* 365, 1045–1049
61. Kylilis, N. *et al.* (2018) Tools for engineering coordinated system behaviour in synthetic microbial consortia. *Nat. Commun.* 9, 2677
62. Goers, L. *et al.* (2014) Co-culture systems and technologies: taking synthetic biology to the next level. *J. R. Soc. Interface* 11, 20140065
63. Miano, A. *et al.* (2020) Inducible cell-to-cell signaling for tunable dynamics in microbial communities. *Nat. Commun.* 11, 1193
64. March, J.C. (2004) Quorum sensing and bacterial cross-talk in biotechnology. *Curr. Opin. Biotechnol.* 15, 495–502
65. Pouzet, S. *et al.* (2020) The promise of optogenetics for bioproduction: dynamic control strategies and scale-up instruments. *Bioengineering (Basel)* 7, 151
66. Zid, B.M. and O'Shea, E.K. (2014) Promoter sequences direct cytoplasmic localization and translation of mRNAs during starvation in yeast. *Nature* 514, 117–121
67. Terzer, M. and Stelling, J. (2008) Large-scale computation of elementary flux modes with bit pattern trees. *Bioinformatics* 24, 2229–2235
68. Chávez-Béjar, M.I. *et al.* (2008) Metabolic engineering of *Escherichia coli* for L-tyrosine production by expression of genes coding for the chorismate mutase domain of the native chorismate mutase-prephenate dehydratase and a cyclohexadienyl dehydrogenase from *Zymomonas mobilis*. *Appl. Environ. Microbiol.* 74, 3284–3290
69. Martínez-Gómez, K. *et al.* (2012) New insights into *Escherichia coli* metabolism: carbon scavenging, acetate metabolism and carbon recycling responses during growth on glycerol. *Microb. Cell Factories* 11, 46
70. Vannelli, T. *et al.* (2007) Production of p-hydroxycinnamic acid from glucose in *Saccharomyces cerevisiae* and *Escherichia coli* by expression of heterologous genes from plants and fungi. *Metab. Eng.* 9, 142–151
71. Delvigne, F. *et al.* (2023) Avoiding the all-or-none response in gene expression during *E. coli* continuous cultivation based on the online monitoring of cell phenotypic switching dynamics. *Methods Mol. Biol.* 2617, 103–120
72. Sassi, H. *et al.* (2019) Segregostat: a novel concept to control phenotypic diversification dynamics on the example of Gram-negative bacteria. *Microb. Biotechnol.* 12, 1064–1075
73. Martinez, J.A. *et al.* (2018) Metabolic modeling and response surface analysis of an *Escherichia coli* strain engineered for shikimic acid production. *BMC Syst. Biol.* 12, 102
74. Edwards, J.S. and Palsson, B.O. (2000) Metabolic flux balance analysis and the in silico analysis of *Escherichia coli* K-12 gene deletions. *BMC Bioinformatics* 1, 1
75. Lendenmann, U. *et al.* (2000) Growth kinetics of Esch*erichia coli* with galactose and several other sugars in carbon-limited chemostat culture. *Can. J. Microbiol.* 46, 72–80
76. Covert, M.W. *et al.* (2001) Regulation of gene expression in flux balance models of metabolism. *J. Theor. Biol.* 213, 73–88
77. Peng, L. *et al.* (2004) Metabolic flux analysis for a ppc mutant *Escherichia coli* based on 13C-labelling experiments together with enzyme activity assays and intracellular metabolite measurements. *FEMS Microbiol. Lett.* 235, 17–23
78. Price, N.D. *et al.* (2004) Genome-scale models of microbial cells: evaluating the consequences of constraints. *Nat. Rev. Microbiol.* 2, 886–897
79. Schmid, J.W. *et al.* (2004) Metabolic design based on a coupled gene expression-metabolic network model of tryptophan production in *Escherichia coli*. *Metab. Eng.* 6, 364–377
80. Visser, D. *et al.* (2004) Optimal re-design of primary metabolism in *Escherichia coli* using linlog kinetics. *Metab. Eng.* 6, 378–390
81. Rizzi, M. *et al.* (1997) In vivo analysis of metabolic dynamics in *Saccharomyces cerevisiae*: II. Mathematical model. *Biotechnol. Bioeng.* 55, 592–608
82. Carlson, R. *et al.* (2002) Metabolic pathway analysis of a recombinant yeast for rational strain development. *Biotechnol. Bioeng.* 79, 121–134
83. Visser, D. *et al.* (2004) Analysis of in vivo kinetics of glycolysis in aerobic *Saccharomyces cerevisiae* by application of glucose and ethanol pulses. *Biotechnol. Bioeng.* 88, 157–167
84. Kesten, D. *et al.* (2015) A new model for the aerobic metabolism of yeast allows the detailed analysis of the metabolic regulation during glucose pulse. *Biophys. Chem.* 206, 40–57
85. Lao-Martil, D. *et al.* (2022) Kinetic modeling of *Saccharomyces cerevisiae* central carbon metabolism: achievements, limitations, and opportunities. *Metabolites* 12, 74
86. Pitkänen, J.-P. *et al.* (2003) Metabolic flux analysis of xylose metabolism in recombinant *Saccharomyces cerevisiae* using continuous culture. *Metab. Eng.* 5, 16–31
87. van Dijken, J.P. *et al.* (2002) Novel pathway for alcoholic fermentation of delta-gluconolactone in the yeast *Saccharomyces bulderi*. *J. Bacteriol.* 184, 672–678
88. Middelhoven, W.J. *et al.* (2000) *Saccharomyces bulderi* sp. nov., a yeast that ferments gluconolactone. *Antonie Van Leeuwenhoek* 77, 223–228
89. Kurtzman, C.P. and Robnett, C.J. (2003) Phylogenetic relationships among yeasts of the '*Saccharomyces* complex' determined from multigene sequence analyses. *FEMS Yeast Res.* 3, 417–432
90. Balarezo-Cisneros, L.N. *et al.* (2023) High quality de novo genome assembly of the non-conventional yeast *Kazachstania bulderi* describes a potential low pH production host for biorefineries. *Commun. Biol.* 6, 918
91. Guidot, D.M. *et al.* (1993) Absence of electron transport (Rho 0 state) restores growth of a manganese-superoxide dismutase-deficient *Saccharomyces cerevisiae* in hyperoxia. Evidence for electron transport as a major source of superoxide generation in vivo. *J. Biol. Chem.* 268, 26699–26703
92. Dirick, L. *et al.* (2014) Metabolic and environmental conditions determine nuclear genomic instability in budding yeast lacking mitochondrial DNA. *G3 (Bethesda)* 4, 411–423
93. Wang, Y. *et al.* (2021) Metabolism characteristics of lactic acid bacteria and the expanding applications in food industry. *Front. Bioeng. Biotechnol.* 9, 612285
94. Tsuji, A. *et al.* (2013) Metabolic engineering of *Lactobacillus plantarum* for succinic acid production through activation of the reductive branch of the tricarboxylic acid cycle. *Enzym. Microb. Technol.* 53, 97–103
95. Poolman, M.G. *et al.* (2004) A method for the determination of flux in elementary modes, and its application to *Lactobacillus rhamnosus*. *Biotechnol. Bioeng.* 88, 601–612
96. Monedero, V. *et al.* (2008) Maltose transport in *Lactobacillus casei* and its regulation by inducer exclusion. *Res. Microbiol.* 159, 94–102
97. Koduru, L. *et al.* (2017) Genome-scale modeling and transcriptome analysis of Leuconostoc mesenteroides unravel the redox governed metabolic states in obligate heterofermentative lactic acid bacteria. *Sci. Rep.* 7, 15721

98. Hickey, M.W. *et al.* (1983) Metabolism of pyruvate and citrate in lactobacilli. *Aust. J. Biol. Sci.* 36, 487–496
99. Hatti-Kaul, R. *et al.* (2018) Lactic acid bacteria: from starter cultures to producers of chemicals. *FEMS Microbiol. Lett.* 365,
100. Filannino, P. *et al.* (2014) Metabolic responses of *Lactobacillus plantarum* strains during fermentation and storage of vegetable and fruit juices. *Appl. Environ. Microbiol.* 80, 2206–2215
101. Bai, D.-M. *et al.* (2004) Strain improvement and metabolic flux analysis in the wild-type and a mutant *Lactobacillus lactis* strain for L(+)-lactic acid production. *Biotechnol. Bioeng.* 88, 681–689
102. Meng, L. *et al.* (2021) The nutrient requirements of *Lactobacillus acidophilus* LA-5 and their application to fermented milk. *J. Dairy Sci.* 104, 138–150
103. Aboulmouna, L. *et al.* (2020) Cybernetic modeling of biological processes in mammalian systems. *Curr. Opin. Chem. Eng.* 30, 120–127
104. Kim, J.I. *et al.* (2008) A hybrid model of anaerobic *E. coli* GJT001: combination of elementary flux modes and cybernetic variables. *Biotechnol. Prog.* 24, 993–1006
105. Namjoshi, A.A. and Ramkrishna, D. (2001) Multiplicity and stability of steady states in continuous bioreactors: dissection of cybernetic models. *Chem. Eng. Sci.* 56, 5593–5607
106. Narang, A. *et al.* (1997) Dynamic analysis of the cybernetic model for diauxic growth. *Chem. Eng. Sci.* 52, 2567–2578
107. Ramkrishna, D. and Song, H.-S. (2012) Dynamic models of metabolism: review of the cybernetic approach. *AIChE J.* 58, 986–997
108. Ramkrishna, D. and Song, H.-S. (2016) Analysis of bioprocesses. Dynamic modeling is a must. *Mater. Today Proc.* 3, 3587–3599
109. Song, H.-S. and Ramkrishna, D. (2009) Reduction of a set of elementary modes using yield analysis. *Biotechnol. Bioeng.* 102, 554–568
110. Shannon, C.E. (1948) A mathematical theory of communication. *Bell Syst. Tech. J.* 27, 379–423
111. Velastegui, E. *et al.* (2023) Is heterogeneity in large-scale bioreactors a real problem in recombinant protein synthesis by *Pichia pastoris*? *Appl. Microbiol. Biotechnol.* 107, 2223–2233

STAR★METHODS

KEY RESOURCES TABLE

Reagent or resource	Source	Identifier
Bacterial and virus strains		
Escherichia coli W3110	ATCC	ATCC BAA-3208
Escherichia coli WHIC+*pJLBaroGfbr*+ and *pTrcTyrCpheACM*	IBT-UNAM Guillermo Gosset Laboratory	N/A
Lactiplantibacillus plantarum	DSMZ	DSM-20174
Deposited data		
Simulation and Analysis files and pipelines repository	This paper	https://gitlab.uliege.be/mipi/published-software/2024-cocultures.
Experimental models: organisms/strains		
Saccharomyces cerevisiae CENPK pchi-eGFP	O'Shea, Denic, and Calarco laboratories	Zid and O'Shea [66]
Saccharomyces cerevisiae PTA 408 +pCA17	IBT-UNAM Guillermo Gosset Laboratory	N/A
Kazachstania bulderi	BCCM	MUCL 38021
Chemicals, peptides, and recombinant proteins		
Biotin	Sigma-Aldrich	B4639
Calcium pantothenate	Sigma-Aldrich	C8731
Nicotinic acid	Sigma-Aldrich	N0761
Myo-inositol	Sigma-Aldrich	I7508
Thiamine HCL	Sigma-Aldrich	T1270
Pyridoxine HCL	Sigma-Aldrich	P6280
Para-aminobenzoic acid	Sigma-Aldrich	A9878
Cobalamin	Sigma-Aldrich	C0884
Folic acid	Sigma-Aldrich	F8758
Yeast Extract	Gibco	212750
Beef Extract	Sigma-Aldrich	B4888
Tryptone	Gibco	211705
L-tyrosine	Sigma-Aldrich	855456
p-coumaric acid	Thermo	A15167
Software and algorithms		
MiPI Biomass Modelling and Simulation toolbox (BMS in mBioMAS)	This paper	https://gitlab.uliege.be/mipi/published-software/mbiomas-core
MiPI Flow Cytometry Analysis toolbox (FCA in mBioMAS)	This paper	https://gitlab.uliege.be/mipi/published-software/mbiomas-core
efmtools	Terzer *et al.* [67]	https://csb.ethz.ch/tools/software/efmtool.html
Others		
Laboratory Twin Bioreactor	BIONET	T1-Twin
BD Accuri Personal Flow Cytometer	BD Biosciences	Accuri C6 Plus
Segregostat	Andrew ZICLER and Frank DELVIGNE MiPI TERRA	https://douile17.github.io/segregostat-ai.github.io/
HPLC-RI	Agilent	Agilent 1200 series

(continued)

Reagent or resource	Source	Identifier
UPLC-Mass	Shimadzu	Nexera 40 Series
HPLC Carbohydrate Analysis column	Aminex	Aminex HPX-87H
UPLC-C18 Analysis column	Waters	ACUITY Premier BEH C18

EXPERIMENTAL MODEL AND STUDY PARTICIPANT DETAILS

Bacterial strains

Escherichia coli W3110 (ATCC BAA-3208), *Lactiplantibacillus plantarum* (DSM-20174) were obtained from ATCC or DSMZ banks, respectively. *Escherichia coli* WHIC+*pJLBaroGfbr*+ and *pTrcTyrCpheACM* was provided by the Instituto de Biotecnología of the Universidad Nacional Autónoma de México (Mexico) [45,68,69]. *Escherichia coli strains* were cultivated in Verduyn medium complemented with vitamins and a carbon source., *L. plantarum* was cultivated in and adapted MRS medium supplemented vitamins with its auxotroph amino acids via yeast extract, Tryptone beef extract and The compositions of these media including the vitamins concentrations can be found in Note S6 in the supplemental information online**.** For pre-cultivations glucose 20 g/L was used for ECO, maltose-glucose 7.5 g/L each for LAB, and glucose-xylose 5 g/L of glucose for ECO*. Ampicillin (50 µg/L) was sterilized by filtration (0.2 µm) and added for ECO* during pre-cultivations for plasmid maintenance. Tetracycline (10 µg/L) was also sterilized by filtration (0.2 µm) and added for ECO*. The pre-cultivations were all performed 37°C and 150 RPM overnight (16 hours) in non-baffled flasks.

Yeast strains

Saccharomyces cerevisiae CENPK *pchi-eGFP* was provided by the O'Shea, Denic, and Calarco laboratories (USA) [66] *Saccharomyces cerevisiae* PTA 408 +*pCA17* was provided by the Instituto de Biotecnología of the Universidad Nacional Autónoma de México (Mexico) [70]. *Kazachstania bulderi* (BEL) was obtained from the BCCM banks. *Saccharomyces strains* were cultivated in Verduyn medium complemented vitamins and carbon source. *Kazachstania* was cultivated in the *L. plantarum* same adapted MRS medium detailed earlier. The compositions of these media can be found in Note S6 in the supplemental information online**.** For pre-cultivations glucose 20 g/l was used for ECO, maltose-glucose 7.5 g/l each for LAB, and glucose-xylose 5 g/L of glucose for ECO*. Ampicillin (50 µg/l) was sterilized by filtration (0.2 µm) and added for SAC* during pre-cultivations for plasmid maintenance. The pre-cultivations were all performed 30°C and 150 RPM overnight (16 hours) in non-baffled flasks.

METHOD DETAILS

Chemostat and Segregostat cultivations

The cultivations were done all at least in duplicate in lab-scale stirred bioreactors (BIONET twin) with a working volume of 1 l and at an initial OD600 of 0.1 and with the corresponding medium (Adapted MRS or Verduyn). A batch phase was before continuous cultures or controlled cultures was used for biomass propagation. These batch phases lasted between 8 and 10 hours with the microorganisms growing in the corresponding medium complemented with carbon sources mix (same as for the pre-cultivations).

Growth data and event fractions were collected based on online FC during the experiments with AAMN [71,72]. Briefly, it consists in an automatic system that takes sample every 15 minutes from the bioreactor, analyses the samples in a flow cytometer (BD Accuri C6plus, Biosciences) and an actuator pulsed different substrates by the means of peristaltic pumps activated on basis of the FC data and a custom MATLAB script. In this case, the actuator was pulsed based on the observed distribution between yeasts and bacteria (see Figure 1 in the main text). The percentage of these two populations activated the addition of one or two carbon sources accordingly. The carbon sources were provided by the feeding at same concentration than during batch phase for chemostat cultivations.

E. coli and *S. cerevisiae* were cultivated at 1000 RPM and 1 VVM with Verduyn medium at a pH of 6.8. The inoculation population ratio for chemostat cultures was 1:1 ECO/SAC (OD600/OD600.), and for the AAMN experiments it was 1:10 ECO/SAC. The latter was done to allow at the end of batch section have proportions near 50% in terms of events fraction and therefore allow control to take actions near the threshold set for the control rule in this case 50%. In chemostat, the feed was set to be 10 g/l of glucose.

For AAMN experiments, the feeding was done with Verduyn medium with no supplemented carbon source, and pulses were set to be either glucose or ethanol each 15 minutes accordingly to the exceeding populations of SAC or ECO, respectively. Dilution rate was set to be 0.1 h^{-1} for both chemostat and AAMN cultivations, while pulses were set to add 0.4 grams of carbon source per pulse of either glucose or ethanol.

L. plantarum and *K. bulderi* were cultivated at a stirring frequency of 400 min^{-1}, an air flow rate of 0.2 VVM with adapted MRS medium at pH of 5.6. The population ratio for inoculation was 1.85:1 LAB/KAZ. The feeding rate was 0.1 h^{-1} after the batch phase to reach around 50% of each strain. In chemostat, the feeding was adapted MRS complemented with 7.5 g/l of maltose and 7.5 g/l of glucose. For AAMN, the feeding was adapted MRS complemented only with maltose (18.375 g/l) and regulation was performed by pulses of glucose, adding 0.15 g in the case of excess of LAB.

Finally, for the production proof of concept utilizing ECO* and SAC*, cultivations were performed at a stirring frequency of 1000 min, an air flow rate of 1 VVM with Verduyn medium at a pH of 6.8 and a dilution rate of 0.1 h^{-1}. The population ratio for inoculation was 1:1 ECO*/SAC*. For the chemostat experimental design (uncontrolled) experiments, three different concentrations were used: 7.5/2.6 g/l GLC/XYL, 6.7/3.3 g/l GLC/XYL and 5.9/4.1 g/l GLC/XYL. For the AAMN experiment, two different runs were performed, and control rule was set to try to maintain the population around 50% by pulsing 0.25 g of either glucose or xylose every 15 minutes in the case of detecting an excess of ECO*or SAC* respectively.

Central carbon metabolic network model construction

In this work, we decided to utilize core central carbon metabolism Network simplifications instead of genome-scale, since all cases would be worked in minimal media with few defined substrates. The central carbon metabolism networks were constructed from the available genome and central core models and metabolic constraints in the literature. Specifically, for ECO and ECO*, the models used were published by Martinez *et al.* [73], Edwards *et al.* [74], Lendenmann *et al.* [75], Covert *et al.* [76], Peng *et al.* [77], Price *et al.* [78], Schmid *et al.* [79], and Visser *et al.* [80]. For SAC and SAC*, we used the metabolic models developed by Rizzi *et al.* [81], Carlson *et al.* [82], Visser *et al.* [83], Kesten *et al.* [84], Lao-Martil *et al.* [85], and Pitkänen *et al.* [86]. For KAZ, we used the metabolic models described in van Dijken *et al.* [87], Middelhoven *et al.*[88], Kurtzman *et al.* [89], Balarezo-Cisneros *et al.* [90], Guidot *et al.* [91], and Dirick *et al.* [92]. Finally, for LAB, we used the metabolic models described in Wang *et al.* [93], Tsuji *et al.* [94], Poolman *et al.* [95], Monedero *et al.* [96], Koduru *et al.* [97], Hickey *et al.* [98], Hatti-Kaul *et al.* [99], Filannino *et al.* [100], Bai et *al.* [101], and Meng *et al.* [102]. Metabolic reactions for each central carbon metabolism were selected including transport reactions and a Biomass composition based mainly on the protein mean content and composition according to each strain bibliography (Note S1 in the supplemental information online). With this selected and curated reaction, a stoichiometric matrix was constructed for each organism.

Elementary mode (EM) analysis

The EM analysis is based on the deconvolution of an organism's metabolic network into flux distribution networks that cannot be further reduced or simplified and that tie the consumption and production of metabolites. Each one of these unique irreducible flux distributions is called an Elementary Mode (EM), and the collection of all EMs then represents all of the organism's metabolic possibilities for a given Metabolic Network. In the case of this work, the curated and simplified core Metabolic Networks were analysed to understand and measure the effects of substrate temporality in the environment toward an organism's niche specialization through phenotypic diversification. The Elementary Flux Distributions Analysis was made with the aid of the program *efmtool* created by Terzer *et al.* [67] and available at https://csb.ethz.ch/tools/software/efmtool.html. This program allowed the construction of the polyhedral cone of solutions for every strain, containing all basal flux distributions in the cell. However, Even with just the core carbon reactions EMs number can reach values of several millions depending mostly on connectivity and reversibility of reactions. Therefore, a reduction was performed by a set of simple constraints that were based on the microorganism pair and the culture conditions. For ECO/SAC and ECO*/SAC* pairs two constraints were used, growing EMs and Aerobic EMs, this is achieved by selecting EMs with biomass production greater than 0 and with Oxygen evolution greater than 0. For the case of LAB/KAZ, the constraints were growing and anaerobic, however, no aerobic EMs were found as expected, given their genome and metabolic capabilities. After this first constrained base reduction, we calculated the yields for each external metabolite in terms of biomass and selected the highest ones for the metabolites that were consumed or produced during the experiments as the Active set of EM distributions. After, we performed a comparison test between each Active set of EMs in the biomass/substrate yield (Y_{max}) space for each of the EMs in

which we compare the yields and derive the aggressivity or competitivity (θ_i) of the strain for each substrate (i) between two different microorganisms (a and b) with the following formula:

$$\theta_i = 1 - \frac{\left|Y^a_{i,\,max} - Y^b_{i,\,max}\right|}{\left(Y^a_{i,\,max} + Y^b_{i,\,max}\right)} \quad [1]$$

This formula effectively compares the capabilities of consumption for each substrate in a state of equality of masses between the strains in a continuous culture where the growth rate is constrained to the dilution rate, it therefore, compares the maximum aggressivity of each strain to dominate the environment. If this index value is 1 it means that both microorganisms could transform the same amount of substrate by unit of biomass and therefore the equilibrium point in a continuous culture would be set by the amount of biomass in the system and their growth rates. Effective changes in the concentration of this metabolite would not allow us to modify this point of equilibrium, or in other words this metabolite would not allow us to exert control in the system composition. Values less than 1 indicate an unbalanced competition in which one of the strains has a better efficiency of substrate conversion and therefore in continuous cultures with dilution rates smaller than the maximum growth rates the strain with a higher index would eventually dominate the environment, the higher is the disparity the faster this fate should occur. Finally, as this value approaches 0 we arrive at a perfect exclusivity state in which only one of the strains can efficiently transform this substrate into biomass. Having alternative indexes for the microorganisms for two different substrates would be the perfect case for controllability as it would allow us to easily feed separately each biomass.

All used organisms curated reaction files and EMs analysis algorithms and pipelines can be found in the repository https://gitlab.uliege.be/mipi/published-software/2024-cocultures.

Dynamic metabolic flux modeling

To model the dynamics of the internal fluxes of the strains and their changes in metabolism, we used a hybrid cybernetic modeling approach. The cybernetic approach has been thoroughly described in the literature [103–109] and a detailed mathematical description can be found in the Note S3 in the supplemental information online. Briefly here, In MONCKS each microorganism is modeled by a set of Monod type ODEs for each selected EM from the active set, and used to calculate the kinetics of biomass kernel sections toward the interaction to a common environmental model 'The reactor'. The latter variables (i.e., Metabolite and biomass concentrations) are used by the microorganism kernels to evaluate their internal regulation variables (cybernetic variables) according to a metabolic objective (i.e., growth rate) and therefore adjust their individual growth, consumption, and production rates. The sum of the effects of all participant cells (kernels) at each time delta is then used in the reactor's next mass balance. This approach allowed us to calculate the approximated fluxes through diverse metabolic processes such as balanced metabolite oxidations, metabolite fermentations, and byproduct consumptions.

The EMs used from simulations were the initially found during the elementary mode analysis. An exception was made for the ECO fermentative modes producing acetate and ethanol from glucose, which were found to be severely overestimated by the highest productive EMs selected during the initial analysis. Therefore, a similar EMs was selected for each fermentation mode which fitted the experimental yields found in ECO axenic cultures, but concomitantly producing other byproducts (i.e., succinate, glycerol). The final EMs used for each strain, ECO, SAC, ECO*, and SAC* were transformed from Yields based on mol as in the stoichiometry reaction networks to g/g based on the formula weights of each metabolite and the summatory of the formula weights times the stoichiometry of the biomass reaction as an estimation for the biomass formula weight in the model. The final used yield values for the models can be found in Note S3 in the supplemental information online.

The calculation of these models was performed with the MONCKS software published in a previous article [13]. In this work, the difference is that the yields and reactions come from an EMs while in the previous work models were made based just on experimental yields and no internal reactions occur. Furthermore, the software and method was polished and translated to python and implemented through a more complete computational toolbox called MiPI Biomass Modelling and Simulation toolbox (mBioMAS) which core is available at https://gitlab.uliege.be/mipi/published-software/mbiomas-core all installation and use information can be obtained there. Simplified diagrams of its working procedures can be found in Note S3 in the supplemental information online**.** The use of this software

is simple and only requires the introduction of the EMs Yields and rates for each strain as well as the initial bioprocess conditions and in the case of the AAMN models the characteristics of the control rules and actuator.

Model parameter approximations were performed by a Montecarlo and Metropolis hasting algorithms to axenic cultures. After this parameter approximation chemostat and AAMN cultures were used as validation for the simulated ECO/SAC systems models. After validation these parameters were used as estimations for the rates of the ECO* and SAC* simulations with different perturbations made to understand the capabilities of stabilization and control. Finally, simulations for the ECO*/SAC* system were performed by changing either the growth rates on each substrate (fitness) and by reducing the byproduct formation (product yield reduction). The simulations by the explained perturbations allowed to study the effects of metabolic niche fitness and metabolic niche size on population stability and controllability. Figures containing the results for all approximations and simulations can be observed in Note S3 in the supplemental information online. All the information regarding the simulations making and future use its available in the repository and all used files and simulation pipelines in this work are available in the repository https://gitlab.uliege.be/mipi/published-software/2024-cocultures.

Competitivity and controllability analysis

In this work we define competitivity as the capability of the strains to allocate certain substrate into their metabolic networks to grow in relationship to the existence of other consuming ones. This can be calculated from the individual Volumetric consumption rates from each individual organisms and comparing it to the total consumption rate. To make this comparison, we decided to use the Shannon's entropy from information theory. This indicator is useful to attest the distribution of a system, and therefore is a good indicator for estimating the effect pulses or environmental changes on the distribution of cellular metabolism. Specifically, to address competitivity (C) and controllability between two different strains in dynamic conditions, we calculated first the relative competitivity of strains similarly to the calculation of θ but considering the growth rates of the microorganisms such that:

$$C = \frac{u^a - u^b}{(u^a + u^b)} \quad [2]$$

It is possible to consider the C across individual substrates or the total competitivity with the actual instantaneous growth rates of the strains. Furthermore we used the Shannon's Entropy to measure the total distribution of metabolic niches across the different strains [110]. For these we use the cybernetic model data that allows us to calculate the volumetric consumption rates for all metabolites across the individual strains. By normalizing each metabolite consumption flow per each strain by the total consumption rate for each substrate s, we can approximate niche participation for each strain (Π_s^a). This niche participation can be set as the probability for a substrate pulse or environmental change would be processed into biomass by each one of the strains and their metabolic states. With this approximation we calculate the partial Entropy (h) of each strain (a and b) for a given substrate (s) in a by the following formulas:

$$h_s^a = -\Pi_s^a \log_2 \Pi_s^a \quad [3]$$

$$h_s^b = -\Pi_s^b \log_2 \Pi_s^b \quad [4]$$

With this information, we can observe the monopoly state of a niche based on the Relative Entropy (K) for each substrate (K_s) by subtracting to 1 the sum of the partial entropies for all strains competing for the substrate:

$$K_s = \frac{\left|H_s^a - H_s^b\right|}{\mathcal{H}_s} \quad [5]$$

This index K_s will be 0 when the probability of the s is the same for it to be consumed by either of the two strains ($\Pi_s^b = \Pi_s^a = 0.5$) and it tends to be 1 whenever the probability of the substrate is to be consumed by one of the strains is closer to 1 (Note S4 in the supplemental information online). In the former case, from a control perspective there is no action possible around the substrate s (pulse or withdrawal) that would allow us to excerpt a meaningful change of the composition of the system. Conversely when this value tends to 1 then changes into this substrate would impact severely the composition of the systems biomass. The analysis of K indexes and the partial entropies can show how well the substrates are being distributed along these microorganisms. Finally, their instantaneous comparison to the Relative competitivity (C) can help us determine which actions (e.g., pulses) could render in better population

control strategies. The behaviour of these indexes can be better observed in the Note S4 in the supplemental information online. The algorithms and pipelines used for the calculation of this indexes can be found in the repository https://gitlab.uliege.be/mipi/published-software/2024-cocultures.

Finally, this entropy analysis was extended to all substrates or Metabolic Niches present in the environment and calculate the total Niche participations and to determine the total dynamic controllability of the system for the chemostat and AAMN experiments and simulations.

QUANTIFICATION AND STATISTICAL ANALYSIS

FC data treatment

Data treatment started by deleting the noise (zero and negative values) and doublets. To address doublet contamination, a linear regression analysis was conducted, correlating the area and height of the forward scattering signal (FSC-A and FSC-H). Data points with Pearson standardized residual values exceeding 2 were identified and eliminated. Samples exhibiting more than 5% doublets or having a total remaining event count below 20,000 were excluded from further analysis. Finally, auto-aggregation was performed by obtaining the mean FSC-A and standard deviation that describes a single cell population. In this case we calculated the Grand Mean and Standard deviations from all samples and assuming that mostly all of them are in a single cell state use this to select events in all samples with values of FSC-A greater than 3 times this standard deviation, therefore with a probability near 97% we can assume this are cells with different morphology than a single cell. This indicates that they can be either supersized or filamented cells or auto-aggerated cells similarly to a method published by Velastegui *et al.* [111] (Note S5 in the supplemental information online). The fractions of events corresponding to each strain, their respective fluorescence and the time of for pump activation were calculated using the MiPI Flow Cytometry Analysis toolbox (mFCAtoolbox) part of the mBioMAS core toolbox available at https://gitlab.uliege.be/mipi/published-software/mbiomas-core all installation and use information can be obtained there. Population fractions were based on gating the yeast populations, defined as events with higher Forward Scatter signal area (FSC-A) than 316227 ($10^{5.5}$) where bacteria were defined as cells with lower values. All FC Data, and treatment algorithms and pipelines can be found in the repository https://gitlab.uliege.be/mipi/published-software/2024-cocultures.

Metabolite analysis

Samples from fermentation experiments were processed for carbon sources (glucose, maltose, xylose and ethanol) measurement by HPLC with an Aminex HPX-87H column (Bio-Rad, Hercules CA, USA) at 45°C and 5 mM Sulfuric acid as mobile phase. An Agilent 1200 Series HPLC system was used with a refraction index detector (RID) at 50°C (Agilent, Santa Clara, CA, USA). The L-tyrosine and p-coumaric acid were detected and quantified by UPLC measurements with Shimadzu Nexera series 40. The flow was 0.6 ml/min and the temperature was 40°C. Detection was done based on a RID and the column was a Water acquity C18 premier 1.7 µm, 2.1 x 50 mm. The analyses were operated with two mobile phases, 0.1% trifluoroacetic acid (TFA) in methanol and 0.1% TFA in water, the distribution table for the mobile phases for the HPLC analyses can be found in Note S6 in the supplemental information online.